COMPARISON OF PREDICTED GROUND-LEVEL AIRBORNE RADIONUCLIDE CONCENTRATIONS TO MEASURED VALUES RESULTING FROM OPERATION OF THE LOS ALAMOS MESON PHYSICS FACILITY

A Thesis

by

WILLIAM VANDERGRIFT HOAK

Submitted to the Office of Graduate Studies of
Texas A&M University
in partial fulfillment of the requirements for the degree of

MASTER OF SCIENCE

May 1993

Major Subject: Health Physics

REPORT DOCUMENTATION PAGE

Form Approved
OMB No 0704-0188

1. AGENCY USE ONLY (Leave blank)

2. REPORT DATE
May 1993

3. REPORT TYPE AND DATES COVERED
THESIS/~~DISSERTATION~~

4. TITLE AND SUBTITLE
Comparison of Predicted Ground-Level Airborne Radio Nuclide Concentrations to measured values resulting from Operations of the Los Alamos Meson Physics Facility

5. FUNDING NUMBERS

6. AUTHOR(S)

Capt William V. Hoak

7. PERFORMING ORGANIZATION NAME(S) AND ADDRESS(ES)

AFIT Student Attending: Texas A&M University

8. PERFORMING ORGANIZATION REPORT NUMBER

AFIT/CI/CIA- 93-010

9. SPONSORING MONITORING AGENCY NAME(S) AND ADDRESS(ES)

AFIT/CI
Wright-Patterson AFB OH 45433-6583

10. SPONSORING MONITORING AGENCY REPORT NUMBER

11. SUPPLEMENTARY NOTES

12a. DISTRIBUTION / AVAILABILITY STATEMENT

Approved for Public Release IAW 190-1
Distribution Unlimited
MICHAEL M. BRICKER, SMSgt, USAF
Chief Administration

12b. DISTRIBUTION CODE

13. ABSTRACT (Maximum 200 words)

14. SUBJECT TERMS

15. NUMBER OF PAGES
72

16. PRICE CODE

17. SECURITY CLASSIFICATION OF REPORT

18. SECURITY CLASSIFICATION OF THIS PAGE

19. SECURITY CLASSIFICATION OF ABSTRACT

20. LIMITATION OF ABSTRACT

COMPARISON OF PREDICTED GROUND-LEVEL AIRBORNE RADIONUCLIDE CONCENTRATIONS TO MEASURED VALUES RESULTING FROM OPERATION OF THE LOS ALAMOS MESON PHYSICS FACILITY

A Thesis

by

WILLIAM VANDERGRIFT HOAK

Submitted to the Office of Graduate Studies of
Texas A&M University
in partial fulfillment of the requirements for the degree of

MASTER OF SCIENCE

May 1993

Major Subject: Health Physics

COMPARISON OF PREDICTED GROUND-LEVEL AIRBORNE RADIONUCLIDE CONCENTRATIONS TO MEASURED VALUES RESULTING FROM OPERATION OF THE LOS ALAMOS MESON PHYSICS FACILITY

A Thesis

by

WILLIAM VANDERGRIFT HOAK

Submitted to Texas A&M University
in partial fulfillment of the requirements
for the degree of

MASTER OF SCIENCE

Approved as to style and content by:

Milton E. McLain
(Chair of Committee)

Gerald A. Schlapper
(Member)

Emile A. Schweikert
(Member)

John W. Poston, Sr.
(Head of Department)

May 1993

Major Subject: Health Physics

ABSTRACT

Comparison of Predicted Ground-Level Airborne Radionuclide Concentrations to Measured Values Resulting from Operation of the Los Alamos Meson Physics Facility. (May 1993)

William Vandergrift Hoak, B.E.E., Villanova University

Chair of Advisory Committee: Dr. Milton E. McLain

A comparison study of measured and predicted downwind radionuclide concentrations from the Los Alamos Meson Physics Facility (LAMPF) was performed. The radionuclide emissions consist primarily of the radioisotopes ^{11}C, ^{13}N, and ^{15}O. The gases, vented to the outside environment by a stack located at the facility, potentially increase the radiation exposure at the facility boundary.

Emission rate, meteorological, and radiation monitoring station data were collected between September 26, 1992 and October 3, 1992. The meteorological and emission data were input to the Clean Air Act Assessment Package-1988 (CAP88-PC) computer code. The downwind radionuclide air concentrations predicted by the code were compared to the air concentrations measured by the monitoring stations. The code was found to slightly overpredict downwind concentrations during unstable atmospheric conditions. For stable atmospheric conditions, the code was not useful for predicting downwind air concentrations. This is thought to be due to an underestimation of hoizontal dispersion.

ACKNOWLEDGMENTS

This work was accomplished under the Service Academy Research Associate Program and funded through the Radioactive Air Emissions Management Program Office at Los Alamos National Laboratory, NM during the summer of 1992. Too many individuals to name graciously found time to provide advice and assistance during the course of the work. Stanley Simmonds and Jerry Miller from the HS-1 group provided valuable advice and encouragement. Larry Andrews and William Wadman took time out of their hectic schedules to help. Special thanks to Don Van Etten and Dave Waechter from the Environmental Management Division for their help with the gamma spectroscopy data. I appreciate the insightful comments and encouragement by my committee, Drs. McLain, Schlapper, and Schweikert.

Finally, I'd like to thank my parents whose love, support, and encouragement has always provided me the confidence to accept a challenge.

TABLE OF CONTENTS

LIST OF TABLES

LIST OF FIGURES

INTRODUCTION

The objective of this thesis is to compare theoretical and measured radionuclide concentrations in air resulting from the radioactive air emissions from the Los Alamos Meson Physics Facility (LAMPF). LAMPF is a half-mile long linear accelerator that provides beams of protons with energies up to 800 megaelectron volts (MeV) at an average current of 1 milliampere. The proton beams are used for research in atomic physics, nuclear chemistry, radiobiology, and condensed matter physics. As this beam of protons passes through air, it activates (transforms stable isotopes into radioactive isotopes) the elements comprising air. These activation products consist primarily of the radioisotopes ^{11}C, ^{13}N, and ^{15}O. The gases, vented to the outside environment by a stack located at the facility, potentially increase the radiation exposure at the facility boundary and are responsible for about 95 percent of the offsite dose caused by Los Alamos National Laboratory. There is considerable interest in verifying the accuracy of the models since LAMPF must cease operation once model projected doses offsite approach regulatory limits.

LAMPF's highest intensity primary beam goes to the meson area to make pions and their progeny (muons and neutrinos). Pions are created when positive-ion proton beam passes thorough two targets in Area A, which is the largest experimental hall. Made of carbon, the targets are contained within a massive concrete shield. From each target, two beam channels deliver particle beams to the experimental caves. The main proton beam continues through the meson

---

This thesis follows the style of *Health Physics*.

hall to the Isotope Production and Radiation Effects Facility and finally is absorbed in the beam stop, where neutrons and neutrinos are produced.

Figure 1 shows the accelerator beam line and the exhaust system. The proton beam is directed into two targets (A-1 and A-2) which are used to produce subatomic particles for use in various experiments. The remaining beam is directed into a beam stop (Shire 1992).

Los Alamos National Laboratory is required by the Environmental Protection Agency (EPA) to maintain a dose of less than 0.1 milliSieverts (mSv) at the boundary of the laboratory (i.e., the maximally exposed member of the general public). In October 1989 the EPA issued final rules for radionuclide emissions to air under 40 CFR Part 61, National Emission Standards for Hazardous Air Pollutants (NESHAPS). Emission monitoring and compliance procedures for Department of Energy (DOE) facilities (40 CFR 61.93(a)) require the use of Clean Air Act Assessment Package-1988 (CAP88-PC) or AIRDOS-PC computer models, or other approved procedures, to calculate effective dose equivalents to members of the public.

The CAP88-PC model uses a modified Gaussian plume equation to estimate the average dispersion of radionuclides released from up to six sources. The sources may be either elevated stacks, such as a smokestack, or uniform area sources. Assessments are done for a circular grid of distances and directions of 30 kilometers around the facility. Because of the simplicity of the model and the conservative assumptions used in CAP88-PC, the EPA claims that the doses estimations are good within a factor of two, normally overprojecting doses for most situtations (EPA 1992).

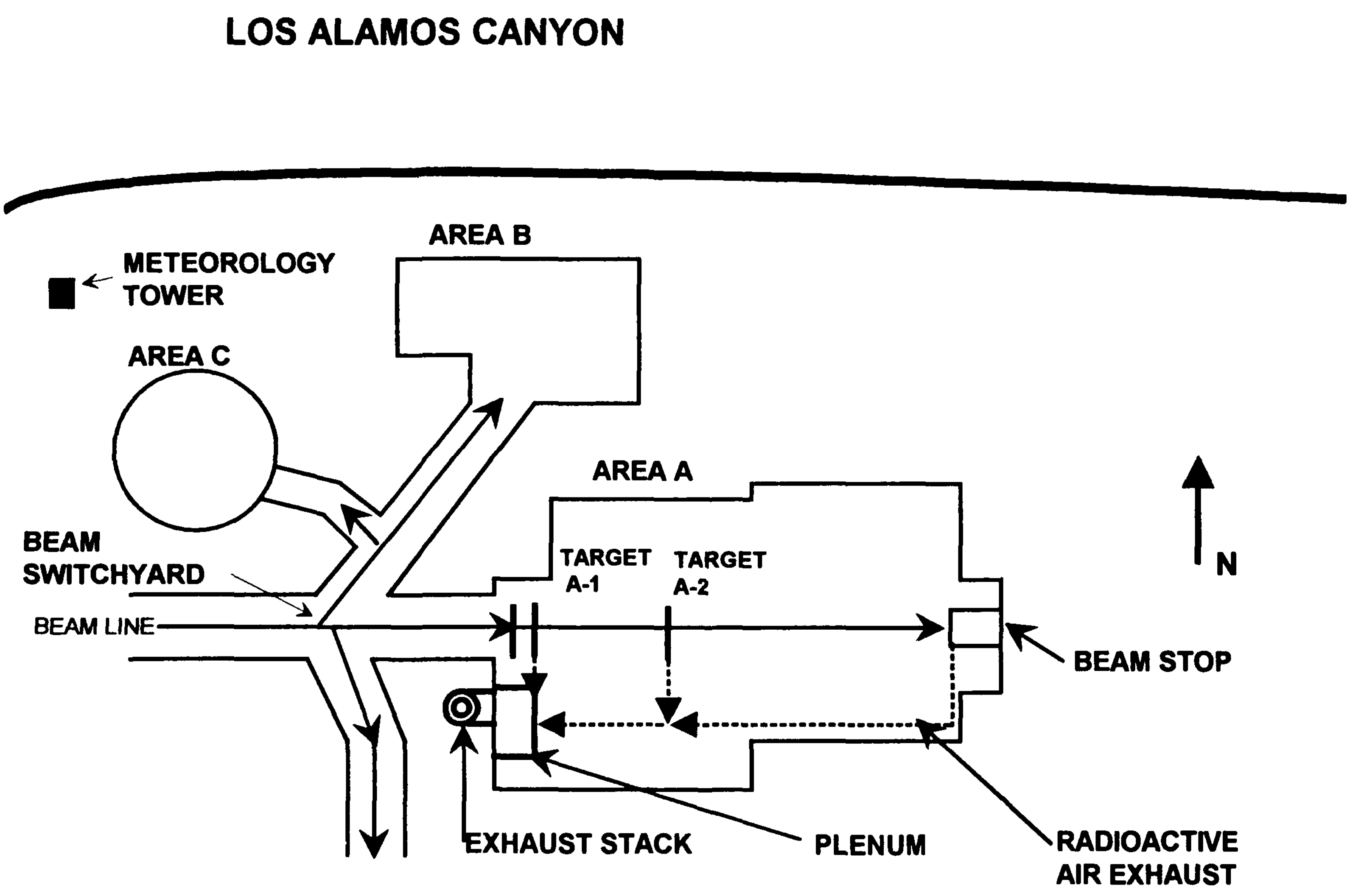

Fig.1. Los Alamos Meson Physics Facility

Because of the above short comings of the model, doses may be significantly overestimated by CAP88-PC model. Additionally, it assumes a that the topology of the area in question is a flat plane. LAMPF is located on the Pajarito Plateau on the eastern flanks of the Jemez Mountains in Northern New Mexico. There are numerous alternating finger mesas and canyons running along the slope line of the plateau. The canyons are 50-100 m deep and 100-200 m wide. LAMPF is located on a mesa top just south of Los Alamos Canyon. The town of Los Alamos is located on the north side of the mesa. This unique topography lends itself to meteorological conditions which are not well addressed by the model. The accelerator in relation to its surrounding is shown in Fig 2.

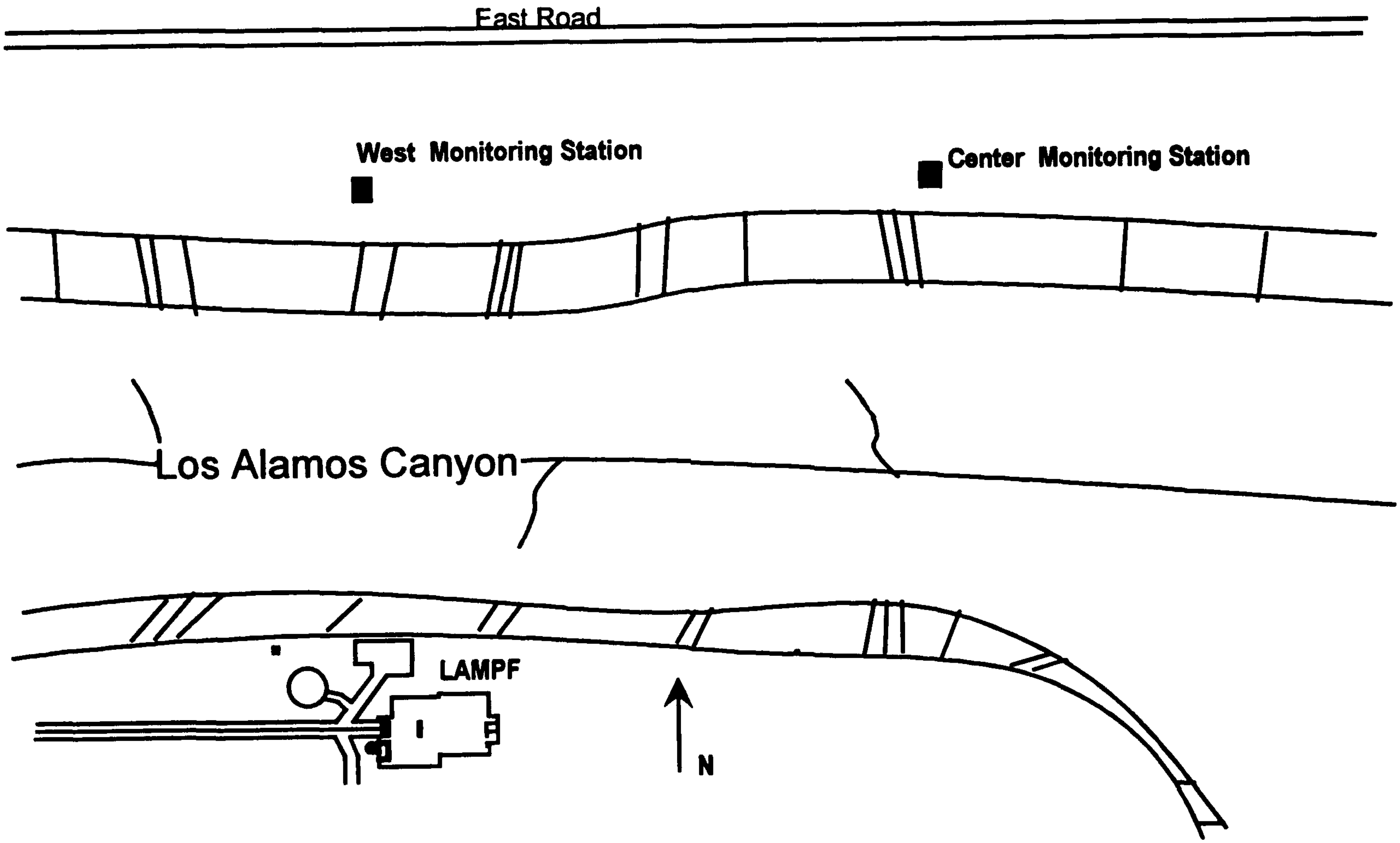

Fig 2. LAMPF and radiation monitoring stations

BACKGROUND

Bowen (Bowen et al. 1987) addressed the accuracy of standard atmospheric models using pressurized ion chambers for population dose estimates in 1985. Both monitoring and modeling of external radiation levels at three locations during 1985 were studied. Predicted daily levels using a simple (infinite cloud) Gaussian model were compared with daily measured values. Predicted values using a more complex finite model were also examined. Average, hourly predicted and measured external radiation levels were compared with each other and in relation to average winds. Accuracy of the model was tested for different times of the day, wind speeds, horizontal wind, and vertical wind. Cumulative external radiation during an 86-day period, as measured by the ion chambers was compared with both the sum of 24-hour estimates and the seasonal form of the model using average winds. Annual model predictions are also compared with TLD measurements.

The simple infinite cloud model was found to overestimate the population dose by over 50% using the ion chambers as a reference. The more complex finite cloud model over estimated the dose by 15%. Bowen found that the models were particularly poor for predicting daytime radiation levels. No consideration was given to amount of radionuclides that are mixed down into the Los Alamos Canyon in transport, or to incorporating wind shear into the calculation. The canyon effect on diffusing radionuclides was not compared using radioactivity levels resulting from transport over the mesa with transport over the canyon.

These models were adequate at the time, because the dose limits were 0.25 mSv and the calculated doses were well below this level. With the recent

change in the dose limit to 0.1 mSv, the current models could under worse case conditions estimate doses in excess of the 0.1 mSv limit, requiring the shutdown of LAMPF for the remainder of the year.

Meteorological Stations

Meteorological data for this study was collected from an instrumented meteorological tower located at the accelerator site (technical area 53). Data on horizontal wind direction and speed are taken at heights of 11.5, 23, and 46 m. Vertical velocity, temperature, solar radiation, relative humidity, and rainfall are also recorded. Data is continuously logged by microprocessors at the tower and averaged over 15 minute intervals. The 15 minute data is retrieved by computer and stored on the Los Alamos central computer system for access by end users.

Radiation Monitoring Stations

To more accurately measure radionuclide activities and compositions, three gamma radiation spectrometers have been setup at the north boundary of the laboratory. These computer controlled instruments have been remotely collecting data on hourly intervals since the last week of August 1992. Data from these spectrometers has significant advantages over the pressurized ion chambers for purposes of this project. The natural background radiation levels at the site boundary range from one to two mSv y^{-1}. Without spectral data, it is very difficult to discern doses on the order of the 0.01 mSv y^{-1}, the level of accuracy required to demonstrate compliance with the law.

The monitoring stations are operated by the Environmental Management Division. Only two stations were operational during the measurement period.

The first station, referred to as the center station, is located 742.8 m from the stack along a 22.5° radial from true north. The second station, referred to as the west station, is located 699.8 m from the stack along a 0° radial (true north). Each station is equipped with a p-type hyperpure germanium (HpGe) gamma spectrometer detector (EG&G Ortec model GEM, 40% nominal efficiency) with cooling provided by electrically powered cryogenic coolers. Data is collected by gamma spectrometry software resident on dedicated personal computers at each station. Calibration of the detector is perfomed using a Europium-152 (^{152}Eu) source placed a various angles along one meter radius arc. A diagram of a station is shown in Figure 3.

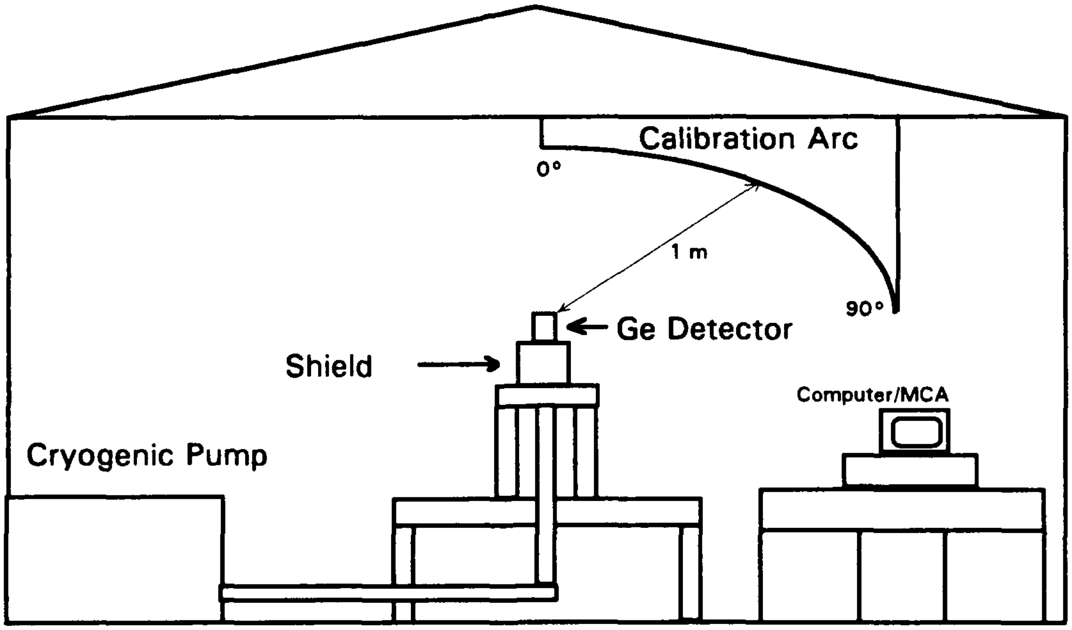

Fig 3: Radiation monitoring station

A typical spectrum collected during the study is shown in Figure 4. The 0.511 MeV annihilation radiation peak is largely due to positron emitting radionuclides released from LAMPF. With the exception of ^{137}Cs, which is the

result of above ground weapons testing, all ot the other nuclides identified are naturally occuring (NCRP 1976). The code READCHN (APPENDIX A) was written to convert the binary data from the multichannel analyzer to American Standards Code for Information Interchange (ASCII) format for analysis.

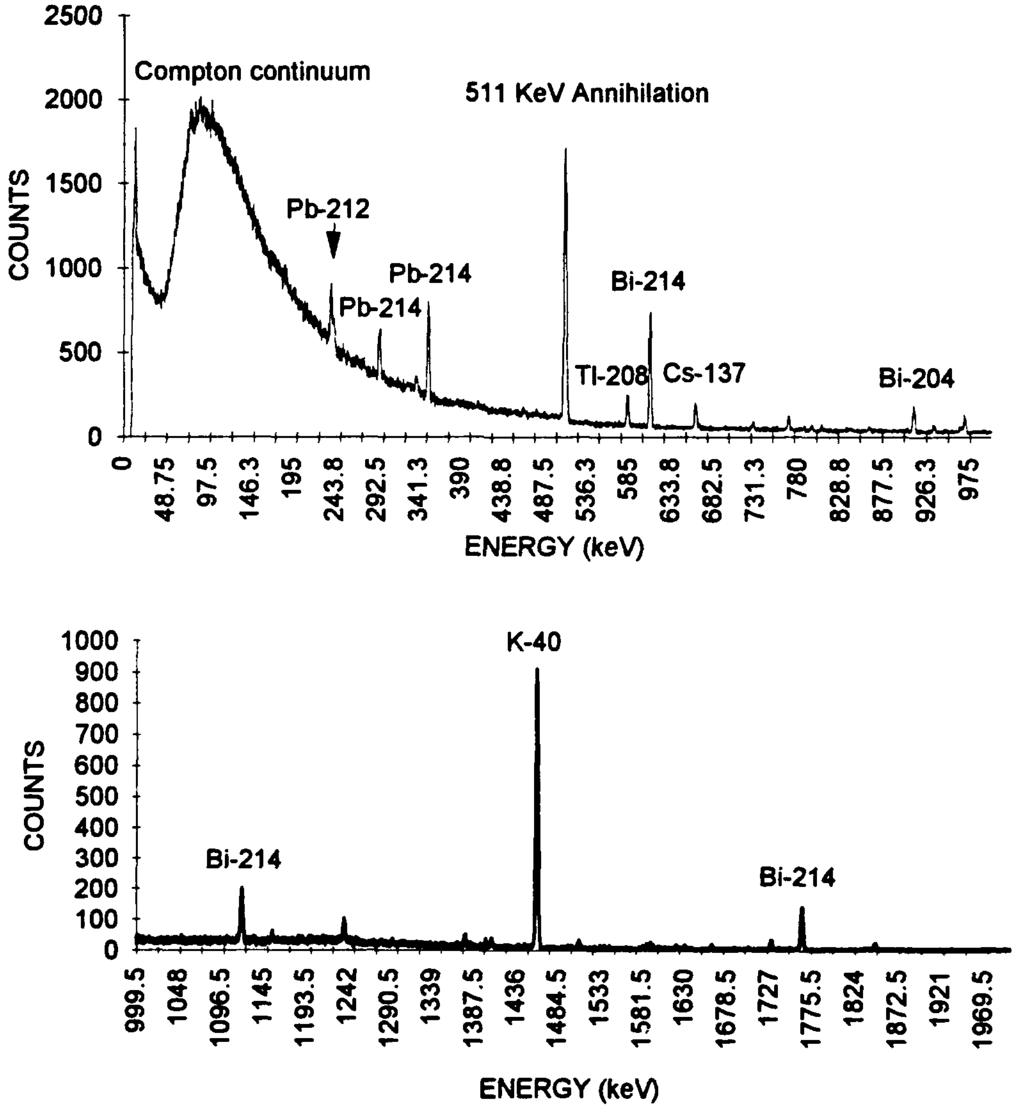

Fig 4. Typical gamma spectrum obtained during monitoring period

Stack Monitoring

The radioactive gases created in the targets and beam stops located in experimental areas A, B, and C are collected and piped to a plenum located at the base of the FE-3 stack. The amount of activity leaving the FE-3 stack is measured using a 5 liter Kanne ionization chamber (Fig. 5) (Engelke and Israel 1973). From the charge collected and an empirically determined activity per charge collected ratio, the total stack gas radionuclide air concentrations in Becquerel m^{-3} (Bq m^{-3}) is calculated. The release rate is then calculated by multiplying the air concentration by the stack flow. Stack velocity is logged by an anemometer placed halfway up the stack. The isotopic constituent (Table 1) measurements of the stack gases are performed on a weekly basis using a germanium-lithium detector gamma spectrometer and a pulse height unfolding algorithm.

Another stack, identified as the FE-2, is located on the site. The output of this stack is less than one percent of the FE-3 stack and was disregarded for purposes of this study.

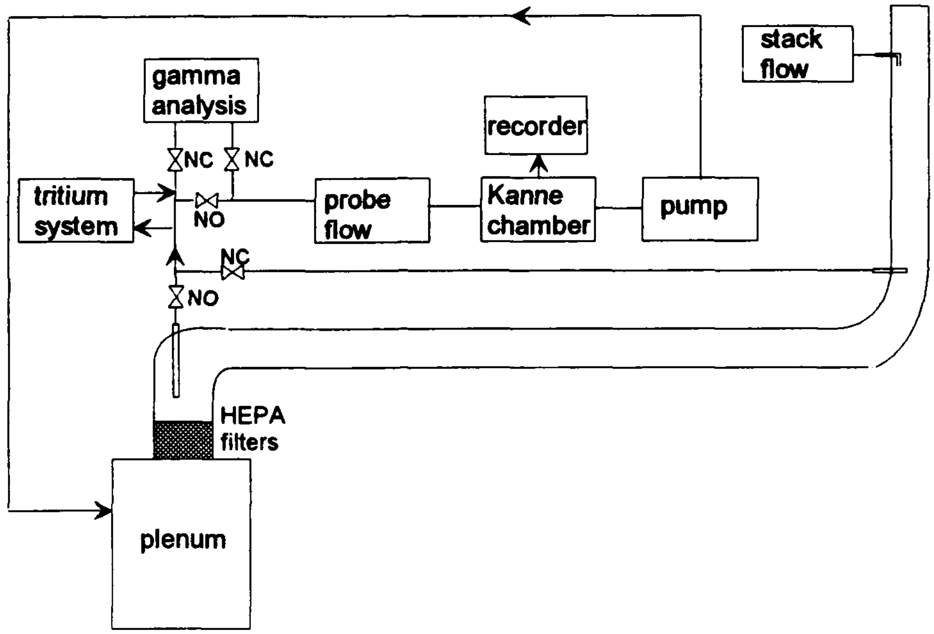

Fig. 5. Radioactive stack gas monitoring system

Table 1. Isotopic composition of exhaust stack*

Isotope	Radioactive half life	Photons emitted MeV (intensity (%))	Percent of total activity released
^{16}N	7.12 s	2.75 (1) 6.13 (69)	1.24
^{10}C	19.3 s	0.511 (200) 0.717 (100)	3.90
^{14}O	1.2 m	0.511 (200) 2.313 (99)	1.57
^{15}O	2.0 m	0.511 (200)	62.29
^{13}N	10.0 m	0.511 (200)	12.46
^{11}C	20.4 m	0.511 (200)	18.23
^{41}Ar	110 m	1.293 (99)	0.31

* Personal communication (1992), Simmonds, S. Los Alamos National Laboratory, NM.

PROCEDURE

Using stack effluent activities obtained from the stack monitoring strip chart recorders, the 15 minute interval meteorological data from the meteorological tower available through the laboratory common file system (CFS), and the data collected on an hourly basis from the two monitoring stations located on the north side of the Los Alamos Canyon, the measured site radionuclide concentrations can be compared to the predicted radionuclide air concentrations from the CAP88-PC code. This code can be tested using the measured meteorological and source term data over a range of conditions.

Meteorological Data

Since the meteorological data is stored in a format which is not amenable to further processing, several computer codes were written as part of this study to aid in the extraction and analysis of the data. APPENDIX B contains the listing for the program METTRAN. This code extracts the required data from the weather file which has been downloaded from the central laboratory computer system and creates a new file with the extracted data. The second code, MET_AVG (APPENDIX C), reads the data file created by METTRAN and calculates one hour averages from the 15 minute data. The one hour data can then be compared with the source term data for that interval and subsequent plume travel near the monitoring stations.

The hourly averaged data is used as input for the CAP88-PC program. CAP88-PC requires that meteorological data be in a stability array format. The stability array is a joint frequency distribution of wind direction and wind speed

for each stability class. The stability class is a typing scheme developed by Pasquill (1961) using the letters A (extremely unstable) through G (moderately stable) to classify the turbulent condition of the atmosphere.

Several methods may be used to derive the stability class. The original work by Pasquill (1961) used solar insolation, cloud cover, and wind speed to determine the stability class. This method suffers from substantial uncertainties, and atmospheric conditions classified as stable may be unstable and vice versa (IAEA 1980). The temperature lapse rate method uses the bulk vertical temperature gradient between two levels in the atmosphere to characterize the stability class. The advantage of this method is in the simplicity of measurement. While it characterizes stable conditions reasonably well, it is not as reliable in unstable conditions (IAEA 1980). A method based on both temperature lapse rate and wind speed (Table 2) is more sensitive since it includes wind speed as an additional variable (Vogt 1977). Additionally, the conditions under which this typing scheme was developed (elevated release and rough terrain) more closely match the situation being modeled.

Table 2. Determination of Pasquill stability class from lapse rate (°C/100 m) and wind speed

	Pasquill Stability Class						
Wind Speed U ($m \cdot s^{-1}$)	$\Delta T/\Delta Z \leq -1.5$	$-1.4 \leq \Delta T/\Delta Z \leq -1.2$	$-1.1 \leq \Delta T/\Delta Z \leq -0.9$	$-0.8 \leq \Delta T/\Delta Z \leq -0.7$	$-0.6 \leq \Delta T/\Delta Z \leq 0.0$	$0.1 \leq \Delta T/\Delta Z \leq 2.0$	$\Delta T/\Delta Z > 2.0$
$U < 1$	A	A	B	C	D	F	F
$1 \leq U < 2$	A	B	B	C	D	F	F
$2 \leq U < 3$	A	B	C	D	D	E	F
$3 \leq U < 5$	B	B	C	D	D	D	E
$5 \leq U < 7$	C	C	D	D	D	D	E
$7 \leq U$	D	D	D	D	D	D	D

Calculation of Air Concentration

Each station was setup to record continuous one hour spectra between September 28 and October 3, 1992. Background spectra were taken during periods when the accelerator was not operating. A shield was placed around the lower portion of the detector in an attempt to minimize the contribution of radionuclides present in the ground to the readings.

Calibration of the detector was accomplished by an ^{152}Eu calibration source. The source was placed at one meter from the detector and spectra collected. The corrected source activity was 3.94 x10^4 Bq on July 7, 1992. Table 3 lists the principle ^{152}Eu photon emissions and their intensities.

The angular dependence of the detector was determined using the ^{152}Eu calibration source at 15° intervals between 0° and 90° along an arc placed one meter from the detector. Figure 6 displays the response of the detector at various angles and energies. The angular dependence is most severe at lower energies and at 60°, but is reasonably flat at energies above 350 keV. The response as a function of energy and angle was determined for the energy of interest (0.511 MeV) by interpolation.

Table 3. ^{152}Eu data

Energy (MeV)	Intensity (%)
0.122	37
0.245	8
0.344	27
0.799	14
0.965	15
1.087	12
1.113	14
1.408	22

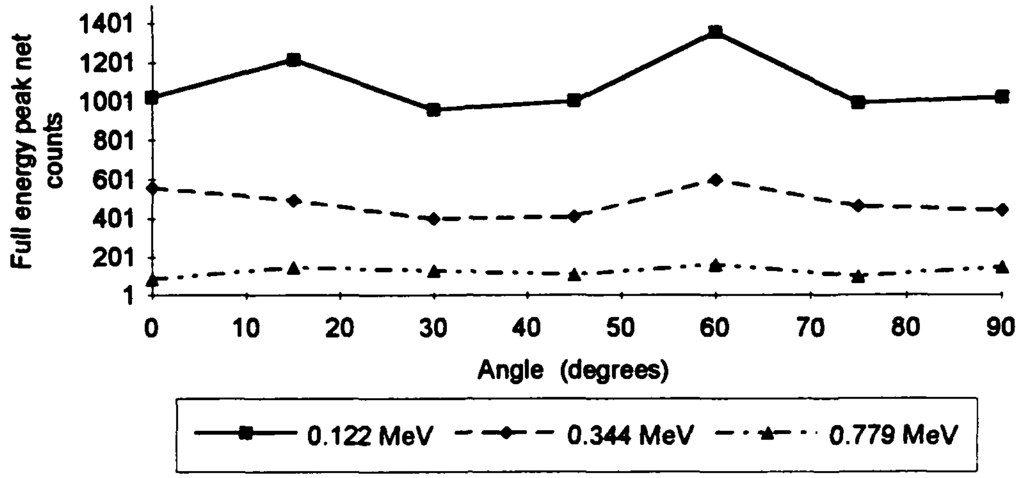

Fig. 6. Response of the HpGe detector vs. angle and energy

Since the quantity of interest is the concentration of radioactive material per unit volume (Bq m^{-3}), the calibration of the detector using a point source has to be related to the irradiation of the detector from a passing cloud. Since all of the nuclides of interest are positron emitters with subsequent annihilation photons, the dose from beta radiation is neglected in the subsequent discussion.

For clouds with dimensions that are small compared to the range of the gamma radiation, a calculation of the gamma dose at a given point must take into account the radiation received from various parts of the cloud. The following equation is suggested by Healy (Healy 1968):

$$ {}_{\gamma}D = \frac{0.1616 \mu \mu_{en} \overline{E}_{\gamma} Q_0 (Q_x / Q_0)(I_1 + kI_2)}{\overline{u}} \tag{1} $$

where:

γD = gamma dose (rads);

μ = total photon absorption coefficient (m^{-1}) in air;

μ_{en} = energy absorption coefficient for photon in air (m^{-1});

E_γ = average photon energy emitted at each disintegration (1.022 Mev dis^{-1});

Q_x = amount of source material (Ci) remaining in the plume after a travel distance x;

Q_0 = amount of source material (Ci) released;

$\overline{U}$ = average wind speed (m/s);

k = $(\mu - \mu_{en})/\mu_{en}$.

I_1 and I_2 are defined as:

$$I_1 = \frac{\bar{u}}{4(2\pi)^{1/2}\mu\sigma_1}\int_0^\infty\int_0^\infty \frac{e^{-\mu r}}{mr} e^{-\left[\frac{(m-r)^2}{2\sigma_1^2}\right]} - e^{-\left[\frac{(m+r)^2}{2\sigma_1^2}\right]} dr \bullet dt \qquad (2)$$

$$I_2 = \frac{\bar{u}}{4(2\pi)^{1/2}\mu\sigma_1}\int_0^\infty\int_0^\infty \frac{\mu e^{-\mu r}}{m} e^{-\left[\frac{(m-r)^2}{2\sigma_1^2}\right]} - e^{-\left[\frac{(m+r)^2}{2\sigma_1^2}\right]} dr \bullet dt \qquad (3)$$

where:

m = distance from the center of the clound to the receptor (m);

σ_l = standard distribution of the material in the cloud (m);

I_1 and I_2 do not have exact solutions. They are evaluated by numerical integration and obtained from published tables.

If the dimensions of a homogeneous cloud of gamma-emitting material are large compared to the distance that the gamma rays travel, an equilibrium condition is acheived. Under these conditions the rate of energy absorption per unit volume is equal to the rate of energy release per unit volume. For a semi–

infinite uniform containing χ Bq m^{-3}, the gamma dose rate (centiGray s^{-1}) to tissue at the cloud center is given by:

$$_{\gamma}D'_{\infty} = 0.0093 E_{\gamma}\chi\left(\frac{\rho_0}{\rho}\right) \quad (4)$$

where ρ_0/ρ is the ratio of the air density at sea level to air density at the point of measurement. For Los Alamos the ratio is 1.3 (Bowen 1992).

The dose to tissue can also be calculated by the relationships:

$$D_{\gamma} = \Psi\left(\frac{\mu_{en}}{\rho}\right) \quad (5)$$

$$\Psi = \frac{(0.511 \cdot \mathrm{MeV})(C_{pp})}{\bar{\varepsilon}_i} \quad (6)$$

where:

Ψ = energy fluence of 0.511 MeV photons crossing the detector (J m^{-2})

μ_{en}/ρ = mass energy attenuation coefficient for 0.511 MeV photon is tissue (cm^2/g)

C_{pp} = number of counts is the 0.511 MeV photopeak of the detector

$\bar{\varepsilon}_i$ = average intrinsic photopeak efficiency of the detector for 0.511 MeV photons

The average photopeak efficiency can be determined from the relationship

$$\bar{\varepsilon}_i = \frac{1}{n} \times \left[\sum_{i=\theta_1}^{\theta_n} \frac{4\pi C_{pp}}{S\Omega_{\theta_i}}\right] \quad (7)$$

where:

S = The total number of photon emitted from the source at a given energy

Ω = The solid angle subtended by the detector at θ; approximated by the frontal area of the detector since the distance between the source is much greater ($>10^3$) than the frontal area of the detector

θ = The angle between the calibration source and vertical axis of the detector

Substituting equations (5) and (6) into equation (4) and solving for χ:

$$\chi = \left[3.69 \times 10^{-6} \mathrm{Bq} \times \mathrm{m}^{-3} \times \mathrm{cnt}^{-1}\right]\left[C_{pp}\right] \qquad (8)$$

CAP88-PC Models

CAP88-PC uses a modified Gaussian plume equation to estimate the average dispersion. The Gaussian plume equation is the mostly common method and produces acceptable results under most conditions.

Plume Rise

Plume rise is modeled by Rupp's (1948) equation for momentum dominated plume rise. The plume rise is added to the actual physical stack height, h, to determine the effective stack height, H.

Rupp's equation for momentum dominated plumes is:

$$\Delta h = \frac{1.5vd}{\mu} \qquad (9)$$

where:

Δh = plume rise (m)

v = effluent stack gas velocity (m $\sec^{-1}$)

d = inside stack diameter (m)

μ = wind velocity (m $\sec^{-1}$)

Plume Dispersion

Plume dispersion is modeled with the Gaussian plume equation of Pasquill (1961) as modified by Gifford (1976):

$$\chi = \frac{Q}{2\pi\sigma_y\sigma_x\mu} e^{[-1/2(y/\sigma_y)^2]} \{e^{[-1/2((z-H)/\sigma_z)^2]} + e^{[-1/2((z+H)/\sigma_z)^2]}\} \quad (10)$$

where:

χ	=	concentration in air at x meters downwind, y meters crosswind, and meters above ground (Ci/m^3)
Q	=	release rate from stack (Ci sec^{-1})
μ	=	wind speed (m sec^{-1})
σ_y	=	horizontal dispersion coefficient (m)
σ_z	=	vertical dispersion coefficient (m)
H	=	effective stack height (m)
y	=	crosswind distance (m)
z	=	vertical distance (m)

The downwind distance x comes into the equation through σ_y and σ_z, which are functions of x as well as the Pasquill atmospheric stability category applicable during emission from the stack.

The equation is applied to ground-level concentrations in air at the plume centerline by setting y and z to zero, which results in:

$$\chi = \frac{Q}{\pi\sigma_y\sigma_z\mu} e^{[-1/2(H/\sigma_z)^2]} \quad (11)$$

CAP88-PC does not provide output of the concentration at a specific point; instead the ground-level concentration in air over a sector of 22.5° is approximated by the expression:

$$\chi_{ave} = f\,\chi \tag{12}$$

where f is the integral of the expression:

$$e^{[-\frac{1}{2}(y/\sigma_y)^2]} \tag{13}$$

in equation (10) from a value of y equals zero to infinity divided by y_s, the value of y at the edge of the 22.5° sector, which is the value of the downwind distance, x, multiplied by the tangent of half the sector angle. The expression is:

$$f = \frac{\int_0^{\infty} e^{[-(1/2/\sigma_y^2)y^2]}\,dy}{y_s} \tag{14}$$

Solving equation (14) and substituting into equation (10) results in the equation for sector-averaged ground level concentration in air:

$$\chi = \frac{Qe^{[-1/2(H/\sigma_z)^2]}}{0.15871\pi x\sigma_z\mu} \tag{15}$$

Plume Depletion

The only mechanism considered for plume depletion in this study was radioactive decay. Depletion is accounted for by substituting a reduced release rate, Q^1, for the original release rate Q for each downwind distance (Slade 1968). The ratio of the reduced release rate to the original is the depletion fraction.

The depletion fraction for radioactive decay is:

$$Q^1 / Q = e^{-\lambda_r t} \tag{16}$$

where:

λ_r = effective decay constant in plume (sec^{-1})

t = time required for plume travel (sec)

Dispersion Coefficients

Horizontal and vertical dispersion coefficients (σ_y and σ_z) used for dispersion calculations in CAP88-PC and for depletion fraction determination are taken from recommendations by G.A. Briggs of the Atmospheric Turbulence and Diffusion Laboratory at Oak Ridge, Tennessee (Moore et al. 1979). The coefficients are different functions of the downwind distance x for each Pasquill stability category for open country conditions (Table 4). Figures 7 and 8 show the plots of these functions. These differ significantly from power-function equation suggested by Slade (1968) and may result in more conservative (higher) dose estimates.

Table 4. Horizontal and vertical dispersion as a function of Pasquill category

Pasquill Category	σ_y (m)	σ_z(m)
A	$0.22\ x\ (1+0.0001x)^{-½}$	$0.20\ x$
B	$0.16\ x\ (1+0.0001x)^{-½}$	$0.12\ x$
C	$0.11\ x\ (1+0.0001x)^{-½}$	$0.08\ x\ (1+0.0002x)^{-½}$
D	$0.08\ x\ (1+0.0001x)^{-½}$	$0.06\ x\ (1+0.0015x)^{-½}$
E	$0.06\ x\ (1+0.0001x)^{-½}$	$0.03\ x\ (1+0.0003x)^{-1}$
F	$0.04\ x\ (1+0.0001x)^{-½}$	$0.016\ x\ (1+0.0003x)^{-1}$
G	calculated by subtracting half the difference between the values for categories E and F from the value for category F	

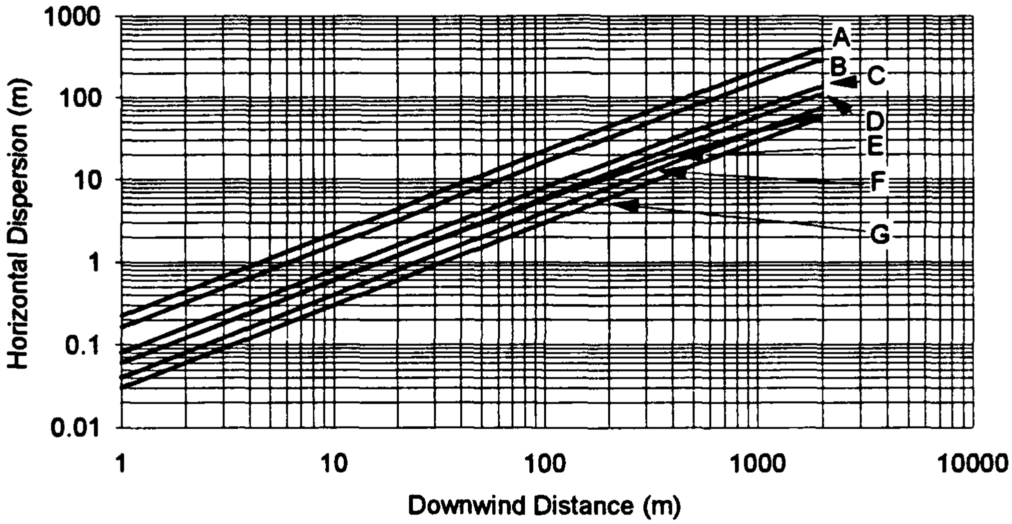

Fig. 7. Horizontal dispersion as a function of downwind distance from the source and Pasquill stability class

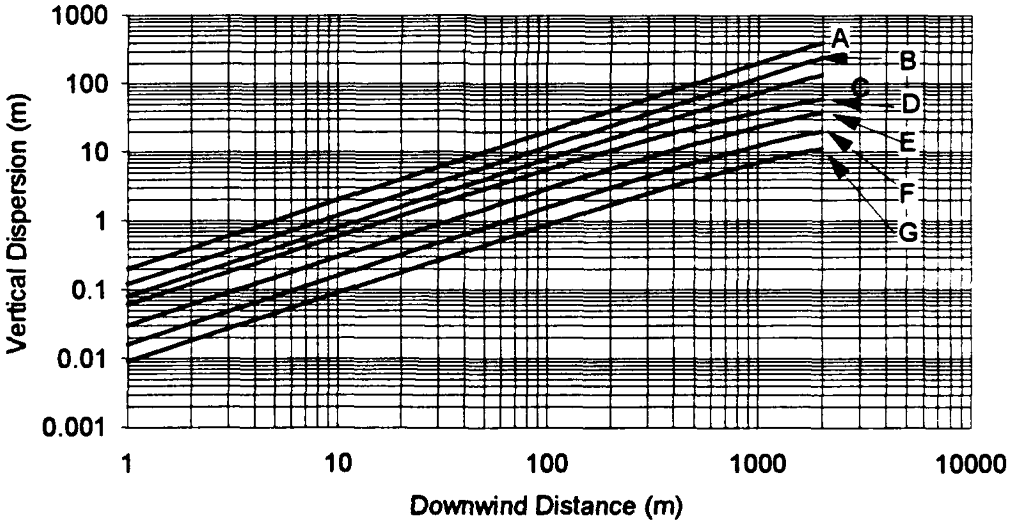

Fig. 8. Vertical dispersion as a function of downwind distance from the source and Pasquill stability class .

RESULTS AND DISCUSSION

In order to correlate the results to different atmospheric conditions, they were divided into atmospheric stability categories A and B, C and D, and E and F. The data were also divided by day and night observations and wind speed intervals.

The A and B category is shown in Fig. 9. The linear regression equation for this data is $y = 1.05 \cdot x$, with $r^2 = 0.57$. Several outlying points near the origin are probably due to varying radiation background levels. The average difference between measured and predicted values is -3.0×10^{-3} Bq m^{-3}. In this case the predicted values slightly overestimate the measured values.

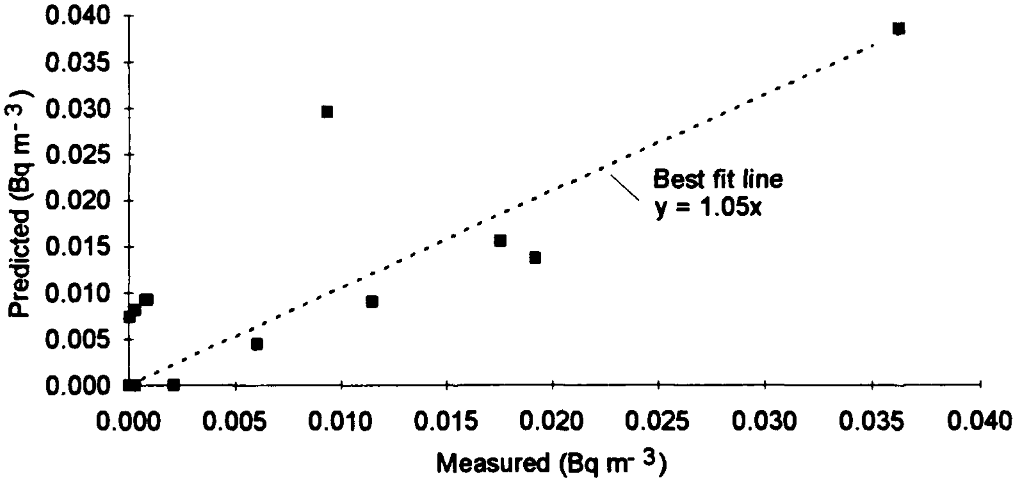

Fig. 9. Measured vs. predicted values for stability classes A and B

Categories C and D are shown in Fig. 10. The data shows poor correlated (r^2=0.02). The average difference between measured and predicted values is

3.0×10^{-3} Bq m^{-3}, with the predicted values underestimating the measured values.

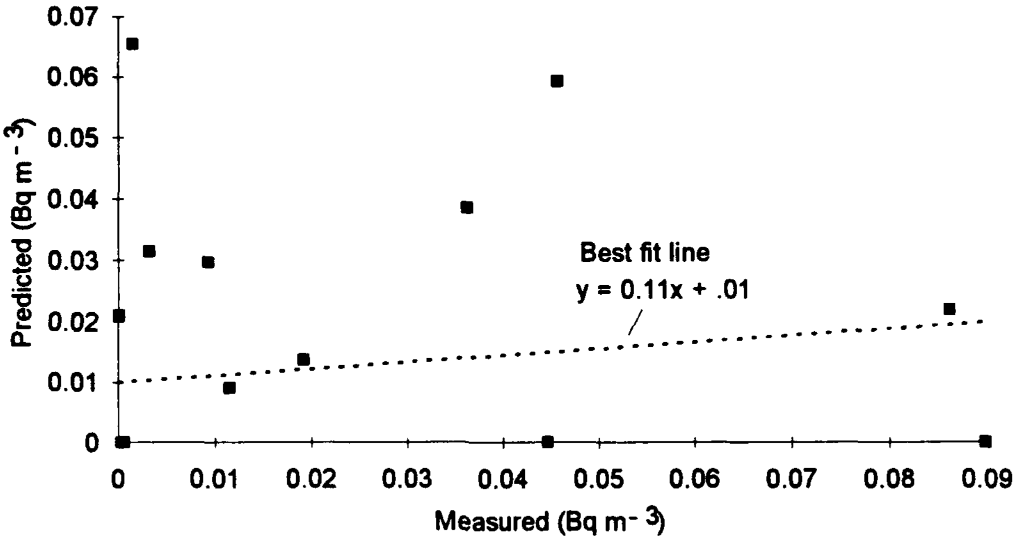

Fig. 10. Measured vs. predicted values for *stability* classes C and D

Stability classes E and F are shown in Fig. 11. The model generally failed to predict most of the measured values leading to the conclusion that the data is uncorrelated ($r^2 \cong 0$). The average difference between measured and predicted values in this case is 2.4×10^{-2} Bq m^{-3}. This result is probably due to an underestimation of the diffusive power of the atmosphere and terrain by the model with increasing atmospheric stability.

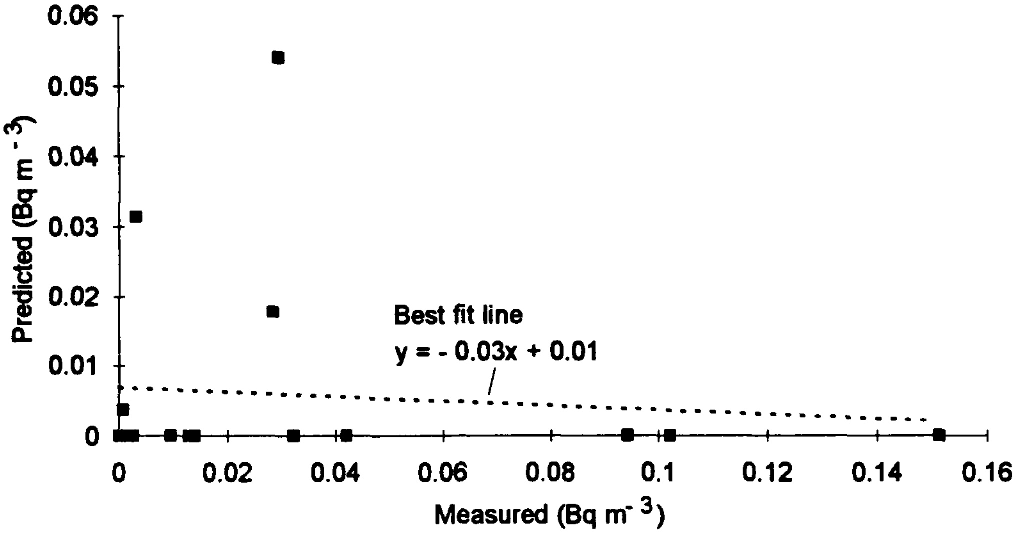

Fig. 11. Measured vs. predicted values for stability classes E and F

The data is divided into day and night values in Figs. 12 and 13. The data is correlates for daytime measurements (y = 0.69, $r^2 = 0.46$). The average difference between measured and predicted values is - 4.0 x 10^{-4} Bq m^{-3}. For nighttime measurements no correlation was found ($r^2 \cong 0$). The results for day and night follow the foregoing discussion for stability classes since unstable atmospheric conditions predominate during the day and stable (atmospheric inversions) during the night.

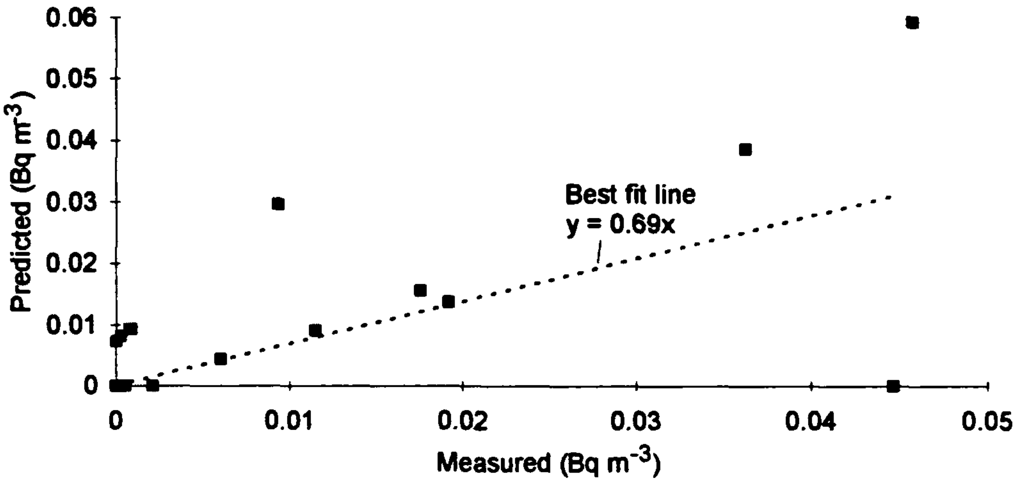

Fig 12. Daytime measured vs. predicted concentrations (r^2=0.46)

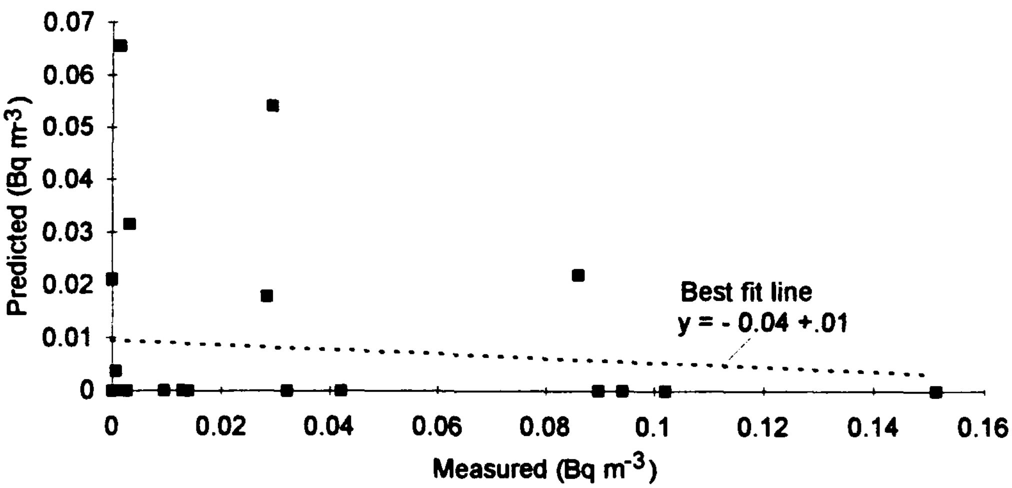

Fig 13. Nighttime measured vs. predicted concentrations (r^2=0.01).

A positive correlation between wind speed and the measured concentrations was found, r^2 = 0.33 and 0.18, for the center and west stations, respectively. Because of the short half-lives of the radioisotopes involved, the higher wind speeds will result in a higher amount of activity in the plume when it reaches the measurement point. This leads to the conclusion that higher

wind speed would increase the exposure at the boundary although they tend to also cause greater dispersion in the plume (wind speed being inversely proportional to concentration in the Gaussian plume equation). A tabulation of the results along with relevant meteorological data is shown in Table 5. The windrose for the survey period is shown in Fig. 14.

Table 5 . Measured and calculated air concentations and meteorological data.

Date	Time	Air Concentration (Bq m^{-3})				Meteorological Parameters			
		West Station		Center Station					
		Measured	CAP88-PC Predicted	Measured	CAP88-PC Predicted	Wind Dir (Degrees)	Wind spd ($m s^{-1}$)	Temp @ 46 m	Temp @ 23 m
269	1400	1.59E-04	0.00E+00	2.77E-04	0.00E+00	286	7.68	21.6	22.1
269	1900	0.00E+00	2.11E-02	2.55E-04	0.00E+00	196	2.85	19.0	19.1
270	0	0.00E+00	0.00E+00	1.11E-04	0.00E+00	189	2.60	13.4	13.5
270	1500	3.62E-02	3.85E-02	1.15E-02	9.07E-03	186	4.68	17.2	17.6
270	2000	1.29E-02	0.00E+00	1.51E-01	0.00E+00	245	5.20	16.9	15.9
271	100	0.00E+00	0.00E+00	3.21E-03	3.15E-02	215	3.30	11.3	11.0
271	600	7.09E-04	3.70E-03	2.94E-02	5.40E-02	204	1.85	10.6	10.5
271	2100	1.38E-02	0.00E+00	9.42E-02	0.00E+00	303	3.65	19.4	18.4
272	1200	1.76E-02	1.55E-02	6.04E-03	4.44E-03	199	5.33	17.6	18.1
272	1700	4.57E-02	5.92E-02	4.47E-02	0.00E+00	180	6.15	19.2	19.5
272	2200	8.98E-02	0.00E+00	8.61E-02	2.18E-02	215	4.48	14.2	14.3
273	300	4.65E-04	0.00E+00	1.47E-03	6.55E-02	212	4.38	11.7	11.4
273	1300	2.10E-03	0.00E+00	3.18E-04	8.14E-03	205	1.95	18.8	19.3
273	1800	5.80E-04	0.00E+00	2.36E-04	0.00E+00	297	5.38	18.3	18.3
274	400	1.40E-02	0.00E+00	9.57E-03	0.00E+00	192	0.55	13.1	13.1
274	900	1.85E-04	0.00E+00	3.32E-05	0.00E+00	40	2.68	12.1	12.4

Table 5. (continued)

Date	Time	Air Concentration (Bq m^{-3})				Meteorological Parameters			
		West Station		Center Station					
		Measured	CAP88-PC Predicted	Measured	CAP88-PC Predicted	Wind Dir (Degrees)	Wind spd (m s^{-1})	Temp @ 46 m	Temp @ 23 m
274	1400	7.87E-04	9.25E-03	7.02E-05	7.40E-03	188	2.85	20.7	21.1
274	1900	3.22E-02	0.00E+00	1.02E-01	0.00E+00	252	4.25	20.1	19.3
275	0	4.43E-04	0.00E+00	2.74E-03	0.00E+00	225	4.23	17.2	16.6
275	1500	8.86E-04	9.25E-03	3.10E-04	0.00E+00	182	2.65	21.4	21.8
276	100	1.35E-03	0.00E+00	2.84E-02	1.78E-02	251	3.68	16.1	15.6
276	1600	1.92E-02	1.37E-02	9.32E-03	2.96E-02	192	4.58	21.6	22.0
276	2100	4.21E-02	0.00E+00	1.19E-03	0.00E+00	243	5.70	18.9	17.9
277	1700	BEAM OFF				197	6.18	20.0	20.4

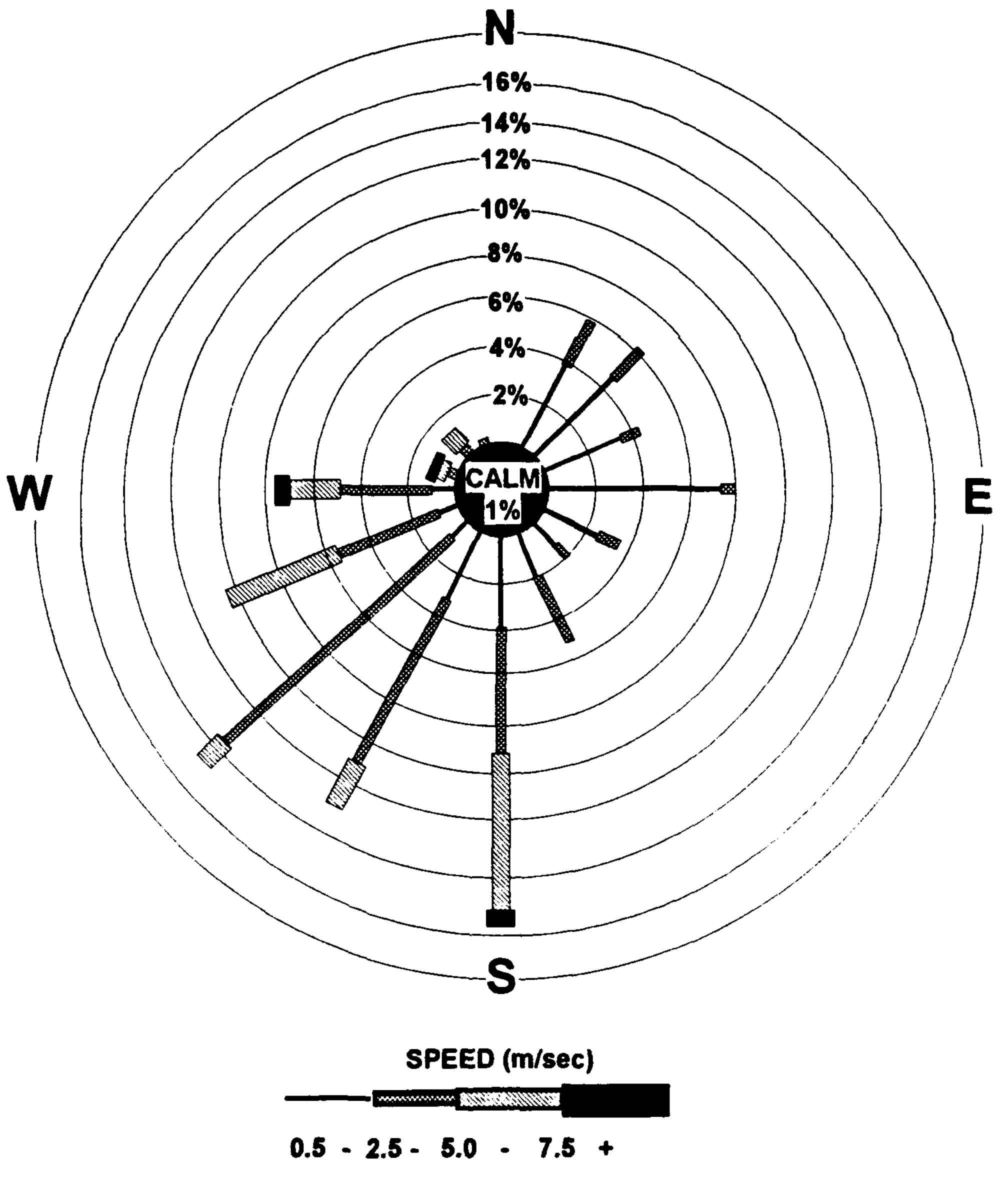

Fig 14. Wind rose from TA-53 tower at 23 m during study period.

CONCLUSIONS

In general, the model slightly overpredicts (5%) downwind concentrations for the unstable atmospheric conditions which generally occur during daytime. The results under these conditions are acceptable considering the nonuniformity of the terrain, variation in the meteorological conditions, and the uncertainties associated in deriving the air concentrations from the gamma spectroscopy data.

For nighttime and stable atmospheric conditions, the model was not useful for predicting the downwind concentrations. This is thought to be due to an underestimation of the dispersion of the atmosphere by the model under these conditions. The model generally did not predict any concentrations in sectors adjacent to the sector in which the wind was primarily blowing for stable atmospheric conditions. This led to a large number of false negatives in the north sector when the wind was primarily blowing from the south-southwest (into the north-northwest sector). The measurement data in these cases shows measurable elevations above background in the north sector.

Nighttime values may also be affected by the lower average wind speeds at night. Bowen (1987) found winds at the East Gate tower, located on the same side of the canyon as the radiation monitoring stations, to be considerably higher than those measured at the LAMPF tower. If the true wind speed is higher than that measured at the LAMPF tower, the downwind concentrations predicted by the model would underestimate the measured concentrations, as is the case.

It is difficult to draw a general conclusion as to whether the dose to an individual would be over- or underestimated from the foregoing discussion. It

depends on his location, the predomininate wind patterns, and atmospheric stability. If data is collected during the entirety of the next accelerator run cycle, the greater volume of data will allow more precision in the comparison of measured and predicted values.

Varying gamma radiation background levels caused significant uncertainties in the data for certain measurements. It would be advisable to take background measurements as close in time to the actual measurements as possible. This is difficult because the winds blow predominately from the south and southwest and there is no control over the source. Statistical confidence could be improved with longer counting times. In some cases, it was difficult to define a peak at 0.511 MeV, even when the wind was blowing into the sector where the measurement was conducted.

FUTURE WORK

All three monitoring stations will be in operation during the next run cycle (May - October 1993). Additionally, weather stations will be installed at each monitoring station, improving knowledge of the micrometeorological conditions. Planned upgrades to the stack monitoring system include logging the output activity in near real time. Currently, only daily output is logged. This introduces error in the source term calculations for periods shorter than one day; the beam current and hence the source output having been found to vary significantly over the course of a day. These upgrades will allow greater data confidence and should be in place for the entire run cycle next year.

An improved method of deriving the air concentration from the gamma spectrum data could be developed. If data on average plume dimensions for each stability class were known, a stability class dependent conversion factor could be developed. A laser identification and ranging system (LIDAR) may be effective in providing more information on plume dimensions. Monte Carlo techniques could then be applied to improve the accuracy of photon fluence estimations at the detectors. Consideration should also be given to using a more powerful dispersion model incorporating local terrain features, such as the Terrain Responsive Atmospheric Code (TRAC) model (Hogdin 1986).

REFERENCES

Bowen, B.M. Los Alamos climatology summary, including latest normals from 1961-1990. Los Alamos, NM: Los Alamos National Laboratory; LA-12232-MS; 1992.

Bowen, B.M.; Dewart J.M.; Fenald F.G. A study of the nocturnal drainage flow over a sloping plateau in north-central New Mexico. Proceedings of second conference on mountain meteorology. American Meteorological Society. 225-232; 1981.

Bowen, B.M.; Olsen, W.A.; Van Etten, D.; Chen, I. Measurement and modeling of external radiation during 1984 from LAMPF atmospheric emissions. Los Alamos, NM: Los Alamos National Laboratory; LA-10766-MS; 1986.

Briggs G.A. Plume rise. Atomic Energy Commission Critical Review Series. Washington, DC: U.S. Government Printing Office; TID 25075; 1969.

Draxler, R.R. Determination of atmospheric diffusion parameters. Atmospheric Environment. 10:99-105; 1976.

Engelke, M.J.; Isreal, H.I. A monitor for radioactive gas in the LAMPF accelerator beam channel. Los Alamos, NM: Los Alamos National Laboratory; LA-5351; 1973.

Gifford, F. Statistical properties of a fluctuation plume model. Advances in Geophysics. 6:117; 1959.

Healy, J.W.; Baker R.E. Radioactive cloud-dose calculations. In: Slade, D.H., ed. Meteorology and atomic energy 1968. Washington, DC: U.S. Atomic Energy Commission; TID 24190; 1968: 251-374.

Hogdin, C.R. Meteorological support at the Rocky Flats Plant. Rocky Flats Plant, CO: Department of Energy Rocky Flats Plant; RFP-4035; 1986.

International Atomic Energy Agency. Atmospheric dispersion in nuclear power plant siting. Vienna: International Atomic Energy Agency; IAEA Safety Series No. 50-SG-S3; 1980.

Moore, D.J. A comparison of trajectories of rising buoyant plumes with theoretical/empirical models. Atmospheric Environment. 8:441; 1979.

National Council on Radiation Protection and Measurements. Environmental radiation measurements. Bethesda, MD: National Council on Radiation Protection and Measurements; NCRP Report No. 50; 1976.

Pasquill, F. The estimation of the dispersion of windborne material. Meteorology Magazine. 90:33; 1961.

Rupp, E.M.; Beall, S.E.; Bornwasser, L.P.; Johnson, D.H. Dilution of stack gases in cross winds. Oak Ridge, TN: U.S. Atomic Energy Commission; AECD-1811; 1948.

Shire, P.R. LAMPF stack emissions calculation. Los Alamos, NM: Los Alamos National Laboratory; Draft report; 1992.

Slade, D.H. Atmospheric dispersion. In: Slade, D.H., ed. Meteorology and atomic energy 1968. Washington, DC: U.S. Atomic Energy Commission; TID 24190; 1968; 85-249.

Turner, D.B. Workbook of atmospheric dispersion estimates. Research Triangle Park, NC: U.S. Environmental Protection Agency, Office of Air Programs; 1970.

U.S. Department of Energy. US Department of Energy Order 5484.1: Chapter III: Effluent and environmental monitoring program requirements. Washington, DC: 1981.

U.S. Environmental Protection Agency. User's guide for CAP88-PC: version 1.0. Las Vegas, NV: US EPA Office of Radiation Programs; 402-B-92-001; 1992.

Vogt, K.J. Empirical investigations of the diffusion of waste air plumes in the atmosphere. Nuclear Technology. 34:51-79; 1977.

SUPPLEMENTAL REFERENCES

Allred, J.C.; Talley, B. LAMPF. Los Alamos, NM: Los Alamos National Laboratory; LA-UR-87-327. 1987.

Attix, F.H. Introduction to radiological physics and dosimetry. New York: John Wiley and Sons; 1986.

Knoll, G.F. Radiation detection and measurement. New York: John Wiley and Sons; 1979.

Prata, S. The Waite group's C++ primer plus. Mill Valley, CA: Waite Group Press; 1991.

APPENDIX A

A LISTING OF THE MCS CODE

```
/******** MCS.C *********************************************************************/
/******** C PROGRAM TO CONVERT MCS DATA TO SINGLE COLUMN **/
/******** AND REMOVE HEADER INFO ******************************************/
/*********15 JUL 92 ******************************************************************/

#include <stdio.h>
#include <string.h>
#include <stdlib.h>
#include <ctype.h>

FILE *f_in, *f_out;
int data[5000];

main()
{
char infile[30], outfile[30];
char line[80], mline[80];
int c,d, index, dummychar;
int i, nl=0, nc=0, channum;

/**** GET INPUT AND OUTPUT FILE NAMES ************/
printf("Program MCS\nReads multichannel scaler data, strips
header,and reformats data\n\n");

        do
          {
                printf("\n Input file name? ");
      gets(infile);
          }
while ((f_in = fopen(infile,"r")) == NULL);

        do
          {
```

```
                printf("\n Output file name? ");
                gets(outfile);
            }
    while ((f_out = fopen(outfile,"w")) == NULL);

        index=0;
      do
      {
       do
       {
/***  READ FIRST LINE OF FILE AND CHECK FOR END OF FILE  ***/

  fgets(line,80, f_in);
  if (feof(f_in)) break;

/* SKIP OVER HEADER */
/** FIRST CHAR OF EVERY DATA LINE CONTAINS <ESC> (027 IN ACSII),
/** SO IF IT DOESN'T IT MUST BE A HEADER LINE **/

          do
            {
   fgets(line,80,f_in);
  } while (line[0]!=27);
          do
            {
                line[0]=' '; /** write over <ESC> character **/

/** SCAN LINE AND EXTRACT DATA ***/
                sscanf(line,"%d %d %d %d %d %d %d %d %d",
                   &channum, &data[index], &data[index+1], &data[index+2],
                   &data[index+3], &data[index+4], &data[index+5],
                   &data[index+6], &data[index+7]);

                if ( channum != index ) puts(line);
```

```
                    index += 8;
                    fgets(line,80,f_in);

        } while(line[0]==27);

        if (ferror(f_in))
                {
         perror("Read Error");
          break;
                }

             if (index > 4088) break;

       }while(!feof(f_in));
            }while(!ferror(f_in));
       /* READY TO WRITE OUT DATA */
       /* INDEX HOLDS # OF DATA POINTS */

            printf("Number of data points is %d\n",index);

            for (i=0; i<index; i++)
        fprintf(f_out, "%d\n",data[i]);

            fclose(f_in);
            fclose(f_out);
       }
```

APPENDIX B

A LISTING OF THE METTRAN CODE

```
//---------------------------------------------------------------------------//
// METTRAN.CPP                                                     //
// C++ PROGRAM TO EXTRACT TA-53 METEROLOGICAL DATA      //
// FROM EM-8 FILES                                                  //
// 7 AUG 92                                                        //
// MODIFIED 30 SEP 92                                              //
//---------------------------------------------------------------------------//

#include <fstream.h>
#include <stdlib.h>
#include <time.h>
#include <stdio.h>
#include <conio.h>

//** CHARACTER VARIABLES TO HOLD INPUT STRINGS **//

 char id1[2], jday[4], time1[5], dum1[4], dir3[4], dir2[4], dir1[4], dum2[4],
   sddir3[4], sddir2[4], sddir1[4], dum3[4], spd3[4], spd2[4], spd1[4],
   dum4[4], sdspd3[4], sdspd2[4], sdspd1[4], dum5[4], w3[4], w2[4], w1[4],
   dum6[4], sdw3[4], sdw2[4], sdw1[4] , line_2[100], line_3[100], line_4[100],
   temp3[4], temp2[4], temp1[4], temp0[4], dummy[80];

 int line_index = 1, count = 1;

// ** FLOATING PNT VARS TO HOLD CONVERTED CHAR STRINGS **//

 float _id1, _jday, _time1, _dum1, _dir3, _dir2, _dir1,
    _sddir3, _sddir2, _sddir1, _spd3,
    _spd2, _spd1, _sdspd3, _sdspd2, _sdspd1,
    _w3, _w2, _w1, _sdw3, _sdw2, _sdw1,
    _temp3, _temp2, _temp1, _temp0;

 int main(int argc, char *argv[])
```

```
//** PASS INPUT, OUTPUT FILES AS PART OF COMMAND LINE **//

 {
   if (argc == 1)
//** QUIT IF NO ARGUMENTS **//
         {
cerr << "ERROR == > Usage: Mettran {input file} {output file}\n";
  exit(1);
         }

   int f_in = 1, f_out = 2;

   ifstream fin(argv[f_in], ios::nocreate);

//** ERROR IF INPUT FILE DOESN'T EXIST  **//

   if (fin.fail())
         {
 cerr << "ERROR ==> input file does not exist \n";
  exit(1);
         }

   ofstream fout(argv[f_out], ios::trunc /*discard contents if file exists*/);

//** ERROR WITH OUTPUT FILE  **//

   if (fout.fail())
         {
 cerr <<"ERROR ==> output file error\n";
  exit(1);
         }

//** OUTPUT FILE HEADER **//
//** APPEND FILE SPECS AND PROCESSING TIME TO HEADER **//
```

```
time_t ltime;   //** TIME FUNCS DEFINED IN  <TIME.H> **//
time(&ltime);

fout << "Input File:\t" << argv[f_in] <<"\n"
    << "Output File:\t" << argv[f_out] <<"\n"
    << ctime( &ltime ) << "\n";

fout  << "jday" <<"\t" << "time" <<"\t"
    << "dir3" <<"\t" << "dir2" <<"\t" <<"dir1"
     <<"\t" << "sddir3" <<"\t" << "sddir2" <<"\t"
     << "sddir1" << "\t";

fout << "spd3" <<"\t" << "spd2" <<"\t" << "spd1"
    <<"\t" << "sdspd3" <<"\t" << "sdspd2" <<"\t"
    << "sdspd1" <<"\t" << "w3" <<"\t" << "w2" <<"\t"
    << "w1" <<"\t" << "sdw3" <<"\t" << "sdw2" <<"\t"
    << "sdw1" <<"\t";

fout << "temp3" <<"\t" <<"temp2" <<"\t"
    << "temp1" <<"\t" << "temp0" <<"\n";

// ** READ LINE FROM INPUT FILE                                    **//
// ** NOTE: BECAUSE OF FILE FORMAT, THE DATA MUST BE READ **//
//**  AS A CHAR STRING FIRST                                 **//
// ** NOTE: GET() APPENDS TERMINATION CHARACTER, SO MAKE IT **//
//**  ONE CHAR BIGGER                                        **//

  while( !( fin.eof() ) )
  {

   fin.get(id1,2).get(jday,4).get(time1,5).get(dum1,4).get(dir3,4).get(dir2,4)
    .get(dir1,4).get(dum2,4).get(sddir3,4).get(sddir2,4).get(sddir1,4)
    .get(dum3,4).get(spd3,4).get(spd2,4).get(spd1,4).get(dum4,4);
```

```
    fin.get(sdspd3,4).get(sdspd2,4).get(sdspd1,4).get(dum5,4).get(w3,4)
     get(w2,4).get(w1,4).get(dum6,4).get(sdw3,4).get(sdw2,4).get(sdw1,4)
     .ignore(1,'/n');
    fin.get(dummy,15).get(temp3,5).get(temp2,5).get(temp1,5).get(temp0,5)
      .ignore(51,'\n');

//** SKIP THIRD DATA LINE                                          **//
    fin.ignore(81,'\n');

//** CONVERT STRINGS TO FLOATING POINT NUMBERS                      **//
//** USING ATOF() FUNCTION FROM STDLIB.H                            **//
//** AND ADJUST FOR DECIMAL PLACE IF NEEDED                         **//

 _id1 = atof (id1);
 _jday = atof (jday);                    // JULIAN DATE
 _time1 = atof (time1);                       // TIME

 _dir3 = atof (dir3);                // WIND DIR @ 46 M AGL
 _dir2 = atof (dir2);                // WIND DIR @ 23 M
 _dir1 = atof (dir1);                // WIND DIR @ 11.5 M
 _sddir3 = atof (sddir3);            // STD DEV OF DIR
 _sddir2 = atof (sddir2);
 _sddir1 = atof (sddir1);

 _spd3= 0.1 * atof (spd3);  // WIND SPEEDS
 _spd2= 0.1 * atof (spd2);
 _spd1= 0.1 * atof (spd1);
 _sdspd3 = 0.1 * atof (sdspd3);    // STD DEV OF WIND SPD
 _sdspd2 = 0.1 * atof (sdspd2);
 _sdspd1 = 0.1 * atof (sdspd1);

 _w3= 0.1 * atof (w3);        // VERTICAL WIND SPEEDS
 _w2= 0.1 * atof (w2);
 _w1= 0.1 * atof (w1);
```

```
_sdw3= 0.01 * atof (sdw3);          // STD DEV VERT WND SPDS
_sdw2= 0.01 * atof (sdw2);
_sdw1= 0.01 * atof (sdw1);

_temp3 = 0.1 * atof (temp3);                 // TEMPERATURES
_temp2 = 0.1 * atof (temp2);
_temp1 = 0.1 * atof (temp1);
_temp0 = 0.1 * atof (temp0);

//** OUTPUT DATA TO USER SPECIFIED FILE **//

fout  << _jday <<"\t" << _time1 <<"\t"
   << _dir3 <<"\t" << _dir2 <<"\t" << _dir1
    <<"\t" << _sddir3 <<"\t" << _sddir2 <<"\t"
    << _sddir1 << "\t";

fout << _spd3 <<"\t" << _spd2 <<"\t" << _spd1
   <<"\t" << _sdspd3 <<"\t" << _sdspd2 <<"\t"
   << _sdspd1 <<"\t"<< _w3 <<"\t" << _w2 <<"\t"
   << _w1 <<"\t" << _sdw3 <<"\t" << _sdw2 <<"\t"
   << _sdw1 <<"\t" << _temp3 <<"\t"<< _temp2 <<"\t"
   << _temp1 <<"\t" << _temp0 <<"\n";
//**  UPDATE INDEX VARIABLES                    **//
line_index = line_index + 3;
count = count + 1;
  }

//**  CLOSE FILES **//

  _fcloseall( );
  return 0;

}
```

APPENDIX C

A LISTING OF MET_AVG CODE

```
//*************************************************************************************//
//** MET_AVG.CPP                                                         *//
//** C++ PROGRAM TO AVERAGE 15 MIN WEATHER DATA OVER *//
//** ONE HOUR INTERVALS                                                  *//
//** 1 OCT 92                                                            *//
//*************************************************************************************//
#include <fstream.h>
#include <stdlib.h>
#include <time.h>
#include <stdio.h>
float _jday[5], _time1[5], _dir3[5], _dir2[5], _dir1[5],
        _sddir3[5], _sddir2[5], _sddir1[5], _spd3[5],
        _spd2[5], _spd1[5], _sdspd3[5], _sdspd2[5],
        _sdspd1[5], _w3[5], _w2[5], _w1[5], _sdw3[5],
        _sdw2[5], _sdw1[5], _temp3[5], _temp2[5], _temp1[5],
        _temp0[5];

//** PASS INPUT, OUTPUT FILES AS PART OF COMMANDI LINE **//

        int main(int argc, char *argv[])

        {
        if (argc == 1)

//** QUIT IF NO ARGUMENTS **//

        {
        cerr << "ERROR == > Usage: Met_avg {input_file}
```

```
        }
        int f_in = 1, f_out = 2;
        ifstream fin(argv[f_in], ios::nocreate);

//** ERROR IF INPUT FILE DOESN'T EXIST**//
        if (fin.fail())
        {
        cerr << "ERROR ==> input file does not exist \n";
        exit(1);
        }

        ofstream fout(argv[f_out], ios::trunc /*discard contents if file exists*/);

//** ERROR IF FILE ALREADY EXISTS **//

        if (fout.fail())
        {
        cerr <<"ERROR ==> output file already exists";
        exit(1);
        }

//** OUTPUT FILE HEADER **//
//** APPEND FILE SPECS AND PROCESSING TIME TO HEADER **//

        time_t ltime;
        time(&ltime);

        fout << "Input File:\t" << argv[f_in] <<"\n"
```

```
<< "Output File:\t" << argv[f_out] <<"\n"
<< ctime( &ltime ) << "\n\n";

fout << "\tTA-53 Weather Data Averaged Over 1 Hour Intervals\n";

fout  << "jday" <<"\t" << "time" <<"\t"
<< "dir3" <<"\t" << "dir2" <<"\t" <<"dir1"
<<"\t" << "sddir3" <<"\t" << "sddir2" <<"\t" << "sddir1" << "\t";

fout << "spd3" <<"\t" << "spd2" <<"\t" << "spd1" <<"\t" << "sdspd3" <<"\t"
<< "sdspd2" <<"\t"   << "sdspd1" <<"\t" << "w3" <<"\t" << "w2" <<"\t"
<< "w1" <<"\t" << "sdw3"    <<"\t" << "sdw2" <<"\t" << "sdw1" <<"\t";

fout << "temp3" <<"\t" <<"temp2" <<"\t"
<< "temp1" <<"\t" << "temp0" <<"\n";

//** INITIALIZE ARRAY **//

for (int j = 0; j < 5; j++)
{
_jday[j] = 0;
_time1[j] = 0;
_dir3[j] = 0;
_dir2[j] = 0;
_dir1[j] = 0;
_sddir3[j] = 0;
_sddir2[j] = 0;
_sddir1[j] = 0;
_spd3[j] = 0;
```

```
        _spd2[j] = 0;
        _spd1[j] = 0;
        _sdspd3[j] = 0;
        _sdspd2[j] = 0;
        _sdspd1[j] = 0;
        _w3[j] = 0;
        _w2[j] = 0;
        _w1[j] = 0;
        _sdw3[j] = 0;
        _sdw2[j] = 0;
        _sdw1[j] = 0;
        _temp3[j] = 0;
        _temp2[j] = 0;
        _temp1[j] = 0;
        _temp0[j] = 0;
        }

//** SKIP OVER 6 HEADER LINES                          **//

        for (int i= 0; i < 6; i++)  fin.ignore(200,'\n');

        while ( !( fin.eof() ) )
        {

                for ( int j = 0; j < 4; j++)
                {
                        fin  >> _jday[j] >> _time1[j]
```

```
>> _dir3[j] >> _dir2[j] >> _dir1[j]
>> _sddir3[j] >> _sddir2[j]
>> _sddir1[j] ;

fin >> _spd3[j] >> _spd2[j] >> _spd1[j]
>> _sdspd3[j] >> _sdspd2[j]
>> _sdspd1[j] >> _w3[j] >> _w2[j]
>> _w1[j] >> _sdw3[j] >> _sdw2[j] >> _sdw1[j] >>
_temp3[j]>> _temp2[j] >> _temp1[j] >> _temp0[j] ;

//** STORE RUNNING SUM IN ARRAY ELEMENT 4 **//

_dir3[4] = _dir3[4] + _dir3[j];
_dir2[4] = _dir2[4] + _dir2[j];
_dir1[4] = _dir1[4] + _dir1[j];
_sddir3[4] = _sddir3[4] + _sddir3[j];
_sddir2[4] = _sddir2[4] + _sddir2[j];
_sddir1[4] = _sddir1[4] + _sddir1[j] ;
_spd3[4] = _spd3[4] + _spd3[j];
_spd2[4] = _spd2[4] + _spd2[j];
_spd1[4] = _spd1[4] + _spd1[j];
_sdspd3[4] = _sdspd3[4] + _sdspd3[j];
_sdspd2[4] = _sdspd2[4] + _sdspd2[j];
_sdspd1[4] = _sdspd1[4] + _sdspd1[j];
_w3[4] = _w3[4]+ _w3[j];
_w2[4] = _w2[4] + _w2[j];
_w1[4] = _w1[4] + _w1[j];
```

```
                _sdw3[4] = _sdw3[4] + _sdw3[j];
                _sdw2[4] = _sdw2[4] + _sdw2[j];
                _sdw1[4] = _sdw1[4] + _sdw1[j];
                _temp3[4] = _temp3[4] + _temp3[j];

}

        fout << _jday[3] <<"\t" << _time1[3]
        <<"\t" << _dir3[4]/4 <<"\t" << _dir2[4]/4 <<"\t" << _dir1[4]/4 <<"\t"

        << _sddir3[4]/4 <<"\t" << _sddir2[4]/4 <<"\t" << _sddir1[4]/4 <<"\t";

        fout << _spd3[4]/4 <<"\t" << _spd2[4]/4 <<"\t" << _spd1[4]/4 <<"\t"
        << _sdspd3[4]/4 <<"\t" << _sdspd2[4]/4 <<"\t" << _sdspd1[4]/4 <<"\t"
        << _w3[4]/4;


         fout <<"\t" <<_w2[4]/4 <<"\t" <<   _w1[4]/4  <<"\t" << _sdw3[4]/4 <<"\t"
        << _sdw2[4]  <<"\t" << _sdw1[4]/4 <<"\t" << _temp3[4]/4 <<"\t"
        << _temp2[4]/4 <<"\t" << _temp1[4]/4 <<"\t" << _temp0[4]/4 << "\n" ;

//** RESET ARRAY ELEMENT 4 TO 0 FOR NEXT HOUR'S DATA    *//
        j = 4;
        _jday[j] = 0;
        _time1[j] = 0;
        _dir3[j] = 0;
        _dir2[j] = 0;
        _dir1[j] = 0;
        _sddir3[j] = 0;
```

```
        _sddir2[j] = 0;
        _sddir1[j] = 0;
        _spd3[j] = 0;
        _spd2[j] = 0;
        _spd1[j] = 0;
        _sdspd3[j] = 0;
        _sdspd2[j] = 0;
        _sdspd1[j] = 0;
        _w3[j] = 0;
        _w2[j] = 0;
        _w1[j] = 0;
        _sdw3[j] = 0;
        _sdw2[j] = 0;
        _sdw1[j] = 0;
        _temp3[j] = 0;
        _temp2[j] = 0;
        _temp1[j] = 0;
        _temp0[j] = 0;

        }

        fcloseall();

    return 0;
    }
```

APPENDIX D

A LISTING OF THE READCHN CODE

```
/*******************************************************************************/
/** READCHN.C:  PROGRAM TO READ AND CONVERT          **/
/** HEADER AND CHANNEL FROM A .CHN FILE              **/
/** MODIFIED FROM MAESTRO II MANUAL CODE             **/
/** 17 AUG 92                                        **/
/*******************************************************************************/

#include <stdio.h>
#include <stdlib.h>
#include <process.h>

#define CHN -1

FILE *f_in, *f_out;

/* PASS INPUT, OUT FILES AS PART OF COMMAND LINE */

int main(int argc, char *argv[])
{
  char acq_time[32];    /* BUFFER FOR TIME AND DATE */
  int f_type;
  unsigned int chan_offset, count, mca_num, num_chans, num_writ, segment;
  long int livetime, realtime, chan_data;

      if (argc == 1 | argc == 0)   /* QUIT IF NO ARGUMENTS */
            {printf( "ERROR == > Usage: READCHN {input_file}
{outputfile}\n");
            exit(1);
            }

/** ERROR IF INPUT FILE DOESN'T EXIST **/
      if((f_in = fopen (argv[1], "rb"))== NULL)
      {
            printf ( "ERROR ==> input file does not exist \n");
```

```
            exit(1);
        }
        else printf("Input file  %s  opened\n", argv[1]);

/** ERROR IF OUPUT FILE ALREADY EXISTS **/
        if (( f_out = fopen (argv[2], "w+"))==NULL)
        {
                printf("ERROR ==> output file already exists\n");
                exit(1);
        }
        else printf("Output file  %s  opened\n", argv[2]);

/** READ AND OUTPUT HEADER INFORMATION FROM .CHN FILE **/

    fread(&f_type,sizeof(int),1,f_in);
    if (f_type != CHN)
        {
          printf("Not a valid file\n");
          exit(1);
        }
    fread(&mca_num,sizeof(int),1,f_in);
    fread(&segment, sizeof(int),1,f_in);
    fread(acq_time+12,sizeof(char),2,f_in);
    fread(&realtime,sizeof(long),1,f_in);
    fread(&livetime,sizeof(long),1,f_in);
    fread(acq_time,sizeof(char),2,f_in);
    fread(acq_time+2,sizeof(char),3,f_in);
    fread(acq_time+5,sizeof(char),3,f_in);
    fread(acq_time+8,sizeof(char),2,f_in);
    fread(acq_time+10,sizeof(char),2,f_in);
    fread(&chan_offset,sizeof(int),1,f_in);
    fread(&num_chans,sizeof(int),1,f_in);
```

```
fprintf(f_out, "TYPE =  %4i MCA # %2i SEGMENT #
            %3i\n",f_type,mca_num,segment);
fprintf(f_out, "realtime = %10li SECONDS, LIVETIME
    = %10li        SECONDS\n", realtime/50, livetime/50);

fprintf(f_out, "DATA COLLECTED AT ");
fwrite(acq_time+8,sizeof(char),2,f_out);
putc(':',f_out);
fwrite(acq_time+10,sizeof(char),2,f_out);
putc(':',f_out);
fwrite(acq_time+12,sizeof(char),2,f_out);

fprintf(f_out, " ON ");
fwrite(acq_time,sizeof(char),2,f_out);
putc('-',f_out);
fwrite(acq_time+2,sizeof(char),3,f_out);
putc('-',f_out);
fwrite(acq_time+5,sizeof(char),2,f_out);
fprintf(f_out,"\nSTARTING CHANNEL = %6i, NUMBER OF
    CHANNELS =        %6i\n\n", chan_offset,num_chans);

/** OUTPUT CHANNEL DATA                    **/
    fprintf(f_out,"Input File: %s\n\n", argv[1]);
    fprintf(f_out,"CHANNEL    DATA\n");
    for (count = 0; count < num_chans; count++)
    {
        fprintf ( f_out, "%7i\t\t",count);
        fread (&chan_data,sizeof(long),1,f_in);
        fprintf ( f_out, "%11i\n",chan_data);
    }
    fcloseall();
}
```

APPENDIX E

EXAMPLE CAPP88-PC OUTPUT

CAPP8 8 - P C

Version 1.00

Clean Air Act Assessment Package - 1988

WEATHER DATA

Non-Radon Individual Assessment

Nov 22, 1992 4:58 pm

Facility: LAMPF

Address:

City: LOS ALAMOS

State: NM Zip:

Source Category: FE-3 Stack

Source Type: Stack

Emission Year: 92

Comments: DOWNWIND CONCENTRATIONS FOR JULIAN DATE 276, TIME 2000 - 2100 hrs

Dataset Name: 276_21

Dataset Date: Nov 22, 1992 4:58 pm

Wind File: WNDFILES\276_21.WND

HARMONIC AVERAGE WIND SPEEDS (WIND TOWARDS)

Wind Dir	Pasquill Stability Class A	B	C	D	E	F	G	Frequency
N	0.000	0.000	0.000	0.000	0.000	0.000	0.000	0.000
NNW	0.000	0.000	0.000	0.000	0.000	0.000	0.000	0.000
NW	0.000	0.000	0.000	0.000	0.000	0.000	0.000	0.000
WNW	0.000	0.000	0.000	0.000	0.000	0.000	0.000	0.000
W	0.000	0.000	0.000	0.000	0.000	0.000	0.000	0.000
WSW	0.000	0.000	0.000	0.000	0.000	0.000	0.000	0.000
SW	0.000	0.000	0.000	0.000	0.000	0.000	0.000	0.000
SSW	0.000	0.000	0.000	0.000	0.000	0.000	0.000	0.000
S	0.000	0.000	0.000	0.000	0.000	0.000	0.000	0.000
SSE	0.000	0.000	0.000	0.000	0.000	0.000	0.000	0.000
SE	0.000	0.000	0.000	0.000	0.000	0.000	0.000	0.000
ESE	0.000	0.000	0.000	0.000	0.000	0.000	0.000	0.000
E	0.000	0.000	0.000	0.000	0.000	0.000	0.000	0.000
ENE	0.000	0.000	0.000	0.000	6.055	0.000	0.000	1.000
NE	0.000	0.000	0.000	0.000	0.000	0.000	0.000	0.000
NNE	0.000	0.000	0.000	0.000	0.000	0.000	0.000	0.000

ARITHMETIC AVERAGE WIND SPEEDS (WIND TOWARDS)

	Pasquill Stability Class						
Dir	A	B	C	D	E	F	G
N	0.000	0.000	0.000	0.000	0.000	0.000	0.000
NNW	0.000	0.000	0.000	0.000	0.000	0.000	0.000
NW	0.000	0.000	0.000	0.000	0.000	0.000	0.000
WNW	0.000	0.000	0.000	0.000	0.000	0.000	0.000
W	0.000	0.000	0.000	0.000	0.000	0.000	0.000
WSW	0.000	0.000	0.000	0.000	0.000	0.000	0.000
SW	0.000	0.000	0.000	0.000	0.000	0.000	0.000
SSW	0.000	0.000	0.000	0.000	0.000	0.000	0.000
S	0.000	0.000	0.000	0.000	0.000	0.000	0.000
SSE	0.000	0.000	0.000	0.000	0.000	0.000	0.000
SE	0.000	0.000	0.000	0.000	0.000	0.000	0.000
ESE	0.000	0.000	0.000	0.000	0.000	0.000	0.000
E	0.000	0.000	0.000	0.000	0.000	0.000	0.000
ENE	0.000	0.000	0.000	0.000	6.302	0.000	0.000
NE	0.000	0.000	0.000	0.000	0.000	0.000	0.000
NNE	0.000	0.000	0.000	0.000	0.000	0.000	0.000

FREQUENCIES OF STABILITY CLASSES (WIND TOWARDS)

Pasquill Stability Class

Dir	A	B	C	D	E	F	G
N	0.0000	0.0000	0.0000	0.0000	0.0000	0.0000	0.0000
NNW	0.0000	0.0000	0.0000	0.0000	0.0000	0.0000	0.0000
NW	0.0000	0.0000	0.0000	0.0000	0.0000	0.0000	0.0000
WNW	0.0000	0.0000	0.0000	0.0000	0.0000	0.0000	0.0000
W	0.0000	0.0000	0.0000	0.0000	0.0000	0.0000	0.0000
WSW	0.0000	0.0000	0.0000	0.0000	0.0000	0.0000	0.0000
SW	0.0000	0.0000	0.0000	0.0000	0.0000	0.0000	0.0000
SSW	0.0000	0.0000	0.0000	0.0000	0.0000	0.0000	0.0000
S	0.0000	0.0000	0.0000	0.0000	0.0000	0.0000	0.0000
SSE	0.0000	0.0000	0.0000	0.0000	0.0000	0.0000	0.0000
SE	0.0000	0.0000	0.0000	0.0000	0.0000	0.0000	0.0000
ESE	0.0000	0.0000	0.0000	0.0000	0.0000	0.0000	0.0000
E	0.0000	0.0000	0.0000	0.0000	0.0000	0.0000	0.0000
ENE	0.0000	0.0000	0.0000	0.0000	1.0000	0.0000	0.0000
NE	0.0000	0.0000	0.0000	0.0000	0.0000	0.0000	0.0000
NNE	0.0000	0.0000	0.0000	0.0000	0.0000	0.0000	0.0000
TOT	0.0000	0.0000	0.0000	0.0000	1.0000	0.0000	0.0000

ADDITIONAL WEATHER INFORMATION

Average Air Temperature: 17.9 degrees C

291.1 K

Precipitation: 0.0 cm/y

Lid Height: 1000 meters

Surface Roughness Length: 0.010 meters

Height Of Wind Measurements: 10.0 meters

Average Wind Speed: 6.302 m/s

Vertical Temperature Gradients:

STABILITY E	0.073 k/m
STABILITY F	0.109 k/m
STABILITY G	0.146 k/m

C A P 8 8 - P C Version 1.00

Clean Air Act Assessment Package1988

CONCENTRATION TABLES

Non-Radon Individual Assessment Nov 22, 1992 4:58 pm

Facility: LAMPF

Address:

City: LOS ALAMOS

State: NM   Zip:

Source Category: FE-3 Stack   Source Type: Stack

Emission Year: 92

Comments: DOWNWIND CONCENTRATIONS FOR JULIAN DATE 276, TIME 2000 - 2100 hrs

Dataset Name: 276_21

Dataset Date: Nov 22, 1992 4:58 pm

Wind File: WNDFILES\276_21.WND

ESTIMATED RADIONUCLIDE CONCENTRATIONS
AT VARIOUS LOCATIONS IN THE ENVIRONMENT

Wind Toward	Distance (meters)	Nuclide	Air Concentration (pCi/m3)	Dry Deposition Rate (pCi/m2/s)	Wet Deposition Rate (pCi/m2/s)	Ground Deposition Rate (pCi/m2/s)
N	700	O-15	0.0E+00	0.0E+00	0.0E+00	0.0E+00
N	700	N-13	0.0E+00	0.0E+00	0.0E+00	0.0E+00
N	700	C-11	0.0E+00	0.0E+00	0.0E+00	0.0E+00
N	743	O-15	0.0E+00	0.0E+00	0.0E+00	0.0E+00
N	743	N-13	0.0E+00	0.0E+00	0.0E+00	0.0E+00
N	743	C-11	0.0E+00	0.0E+00	0.0E+00	0.0E+00
NNW	700	O-15	0.0E+00	0.0E+00	0.0E+00	0.0E+00
NNW	700	N-13	0.0E+00	0.0E+00	0.0E+00	0.0E+00
NNW	700	C-11	0.0E+00	0.0E+00	0.0E+00	0.0E+00
NNW	743	O-15	0.0E+00	0.0E+00	0.0E+00	0.0E+00
NNW	743	N-13	0.0E+00	0.0E+00	0.0E+00	0.0E+00
NNW	743	C-11	0.0E+00	0.0E+00	0.0E+00	0.0E+00
NW	700	O-15	0.0E+00	0.0E+00	0.0E+00	0.0E+00
NW	700	N-13	0.0E+00	0.0E+00	0.0E+00	0.0E+00
NW	700	C-11	0.0E+00	0.0E+00	0.0E+00	0.0E+00
NW	743	O-15	0.0E+00	0.0E+00	0.0E+00	0.0E+00
NW	743	N-13	0.0E+00	0.0E+00	0.0E+00	0.0E+00
NW	743	C-11	0.0E+00	0.0E+00	0.0E+00	0.0E+00
WNW	700	O-15	0.0E+00	0.0E+00	0.0E+00	0.0E+00
WNW	700	N-13	0.0E+00	0.0E+00	0.0E+00	0.0E+00
WNW	700	C-11	0.0E+00	0.0E+00	0.0E+00	0.0E+00
				Dry	Wet	Ground

Wind Toward	Distance (meters)	Nuclide	Air Concentration (pCi/m3)	Deposition Rate (pCi/m2/s)	Deposition Rate (pCi/m2/s)	Deposition Rate (pCi/m2/s)
WNW	743	O-15	0.0E+00	0.0E+00	0.0E+00	0.0E+00
WNW	743	N-13	0.0E+00	0.0E+00	0.0E+00	0.0E+00
WNW	743	C-11	0.0E+00	0.0E+00	0.0E+00	0.0E+00
W	700	O-15	0.0E+00	0.0E+00	0.0E+00	0.0E+00
W	700	N-13	0.0E+00	0.0E+00	0.0E+00	0.0E+00
W	700	C-11	0.0E+00	0.0E+00	0.0E+00	0.0E+00
W	743	O-15	0.0E+00	0.0E+00	0.0E+00	0.0E+00
W	743	N-13	0.0E+00	0.0E+00	0.0E+00	0.0E+00
W	743	C-11	0.0E+00	0.0E+00	0.0E+00	0.0E+00
WSW	700	O-15	0.0E+00	0.0E+00	0.0E+00	0.0E+00
WSW	700	N-13	0.0E+00	0.0E+00	0.0E+00	0.0E+00
WSW	700	C-11	0.0E+00	0.0E+00	0.0E+00	0.0E+00
WSW	743	O-15	0.0E+00	0.0E+00	0.0E+00	0.0E+00
WSW	743	N-13	0.0E+00	0.0E+00	0.0E+00	0.0E+00
WSW	743	C-11	0.0E+00	0.0E+00	0.0E+00	0.0E+00
SW	700	O-15	0.0E+00	0.0E+00	0.0E+00	0.0E+00
SW	700	N-13	0.0E+00	0.0E+00	0.0E+00	0.0E+00
SW	700	C-11	0.0E+00	0.0E+00	0.0E+00	0.0E+00
SW	743	O-15	0.0E+00	0.0E+00	0.0E+00	0.0E+00
SW	743	N-13	0.0E+00	0.0E+00	0.0E+00	0.0E+00
SW	743	C-11	0.0E+00	0.0E+00	0.0E+00	0.0E+00
SSW	700	O-15	0.0E+00	0.0E+00	0.0E+00	0.0E+00
SSW	700	N-13	0.0E+00	0.0E+00	0.0E+00	0.0E+00
SSW	700	C-11	0.0E+00	0.0E+00	0.0E+00	0.0E+00
SSW	743	O-15	0.0E+00	0.0E+00	0.0E+00	0.0E+00
SSW	743	N-13	0.0E+00	0.0E+00	0.0E+00	0.0E+00

ESTIMATED RADIONUCLIDE CONCENTRATIONS
AT VARIOUS LOCATIONS IN THE ENVIRONMENT

Wind Toward	Distance (meters)	Nuclide	Air Concentration (pCi/m3)	Dry Deposition Rate (pCi/m2/s)	Wet Deposition Rate (pCi/m2/s)	Ground Deposition Rate (pCi/m2/s)
SSW	743	C-11	0.0E+00	0.0E+00	0.0E+00	0.0E+00
S	700	O-15	0.0E+00	0.0E+00	0.0E+00	0.0E+00
S	700	N-13	0.0E+00	0.0E+00	0.0E+00	0.0E+00
S	700	C-11	0.0E+00	0.0E+00	0.0E+00	0.0E+00
S	743	O-15	0.0E+00	0.0E+00	0.0E+00	0.0E+00
S	743	N-13	0.0E+00	0.0E+00	0.0E+00	0.0E+00
S	743	C-11	0.0E+00	0.0E+00	0.0E+00	0.0E+00
SSE	700	O-15	0.0E+00	0.0E+00	0.0E+00	0.0E+00
SSE	700	N-13	0.0E+00	0.0E+00	0.0E+00	0.0E+00
SSE	700	C-11	0.0E+00	0.0E+00	0.0E+00	0.0E+00
SSE	743	O-15	0.0E+00	0.0E+00	0.0E+00	0.0E+00
SSE	743	N-13	0.0E+00	0.0E+00	0.0E+00	0.0E+00
SSE	743	C-11	0.0E+00	0.0E+00	0.0E+00	0.0E+00
SE	700	O-15	0.0E+00	0.0E+00	0.0E+00	0.0E+00
SE	700	N-13	0.0E+00	0.0E+00	0.0E+00	0.0E+00
SE	700	C-11	0.0E+00	0.0E+00	0.0E+00	0.0E+00
SE	743	O-15	0.0E+00	0.0E+00	0.0E+00	0.0E+00
SE	743	N-13	0.0E+00	0.0E+00	0.0E+00	0.0E+00
SE	743	C-11	0.0E+00	0.0E+00	0.0E+00	0.0E+00
ESE	700	O-15	0.0E+00	0.0E+00	0.0E+00	0.0E+00
ESE	700	N-13	0.0E+00	0.0E+00	0.0E+00	0.0E+00
ESE	700	C-11	0.0E+00	0.0E+00	0.0E+00	0.0E+00
ESE	743	O-15	0.0E+00	0.0E+00	0.0E+00	0.0E+00

Wind Toward	Distance (meters)	Nuclide	Air Concentration (pCi/m3)	Dry Deposition Rate (pCi/m2/s)	Wet Deposition Rate (pCi/m2/s)	Ground Deposition Rate (pCi/m2/s)
ESE	743	N-13	0.0E+00	0.0E+00	0.0E+00	0.0E+00
ESE	743	C-11	0.0E+00	0.0E+00	0.0E+00	0.0E+00
E	700	O-15	0.0E+00	0.0E+00	0.0E+00	0.0E+00
E	700	N-13	0.0E+00	0.0E+00	0.0E+00	0.0E+00
E	700	C-11	0.0E+00	0.0E+00	0.0E+00	0.0E+00
E	743	O-15	0.0E+00	0.0E+00	0.0E+00	0.0E+00
E	743	N-13	0.0E+00	0.0E+00	0.0E+00	0.0E+00
E	743	C-11	0.0E+00	0.0E+00	0.0E+00	0.0E+00
ENE	700	O-15	1.9E+00	3.4E-07	0.0E+00	3.4E-07
ENE	700	N-13	6.3E-01	1.1E-07	0.0E+00	1.1E-07
ENE	700	C-11	9.8E-01	1.8E-07	0.0E+00	1.8E-07
ENE	743	O-15	1.7E+00	3.1E-07	0.0E+00	3.1E-07
ENE	743	N-13	5.8E-01	1.0E-07	0.0E+00	1.0E-07
ENE	743	C-11	9.1E-01	1.6E-07	0.0E+00	1.6E-07
NE	700	O-15	0.0E+00	0.0E+00	0.0E+00	0.0E+00
NE	700	N-13	0.0E+00	0.0E+00	0.0E+00	0.0E+00
NE	700	C-11	0.0E+00	0.0E+00	0.0E+00	0.0E+00
NE	743	O-15	0.0E+00	0.0E+00	0.0E+00	0.0E+00
NE	743	N-13	0.0E+00	0.0E+00	0.0E+00	0.0E+00
NE	743	C-11	0.0E+00	0.0E+00	0.0E+00	0.0E+00
NNE	700	O-15	0.0E+00	0.0E+00	0.0E+00	0.0E+00
NNE	700	N-13	0.0E+00	0.0E+00	0.0E+00	0.0E+00
NNE	700	C-11	0.0E+00	0.0E+00	0.0E+00	0.0E+00
NNE	743	O-15	0.0E+00	0.0E+00	0.0E+00	0.0E+00

ESTIMATED RADIONUCLIDE CONCENTRATIONS
AT VARIOUS LOCATIONS IN THE ENVIRONMENT

Wind Toward	Distance (meters)	Nuclide	Air Concentration (pCi/m3)	Dry Deposition Rate (pCi/m2/s)	Wet Deposition Rate (pCi/m2/s)	Ground Deposition Rate (pCi/m2/s)
NNE	743	N-13	0.0E+00	0.0E+00	0.0E+00	0.0E+00
NNE	743	C-11	0.0E+00	0.0E+00	0.0E+00	0.0E+00

VITA

William Vandergrift Hoak was born in Harrisburg, Pennsylvania in 1963. He received a Bachelor of Electrical Engineering from Villanova University in May of 1986. He was subsequently commissioned a Second Lieutenant in the United States Air Force. Entering active duty in December 1986, he was assigned to the Radiation Services Division of the Air Force Occupational and Environmental Health Laboratory, Brooks Air Force Base, Texas.

After serving as an Environmental Radiation Consultant and Chief, Instrumentation and Calibration Services at the laboratory, Captain Hoak was selected for graduate degree in Health Physics under an Air Force Institute of Technology graduate education program in August of 1990. He is a member of the Health Physics Society. His permanent mailing address is:

William V. Hoak

c/o Walker V. Hoak

107 North 34th St

Harrisburg, PA. 17109-3605